iScience

CellPress
OPEN ACCESS

Article

The scaffolding function of LSD1/KDM1A reinforces a negative feedback loop to repress stem cell gene expression during primitive hematopoiesis

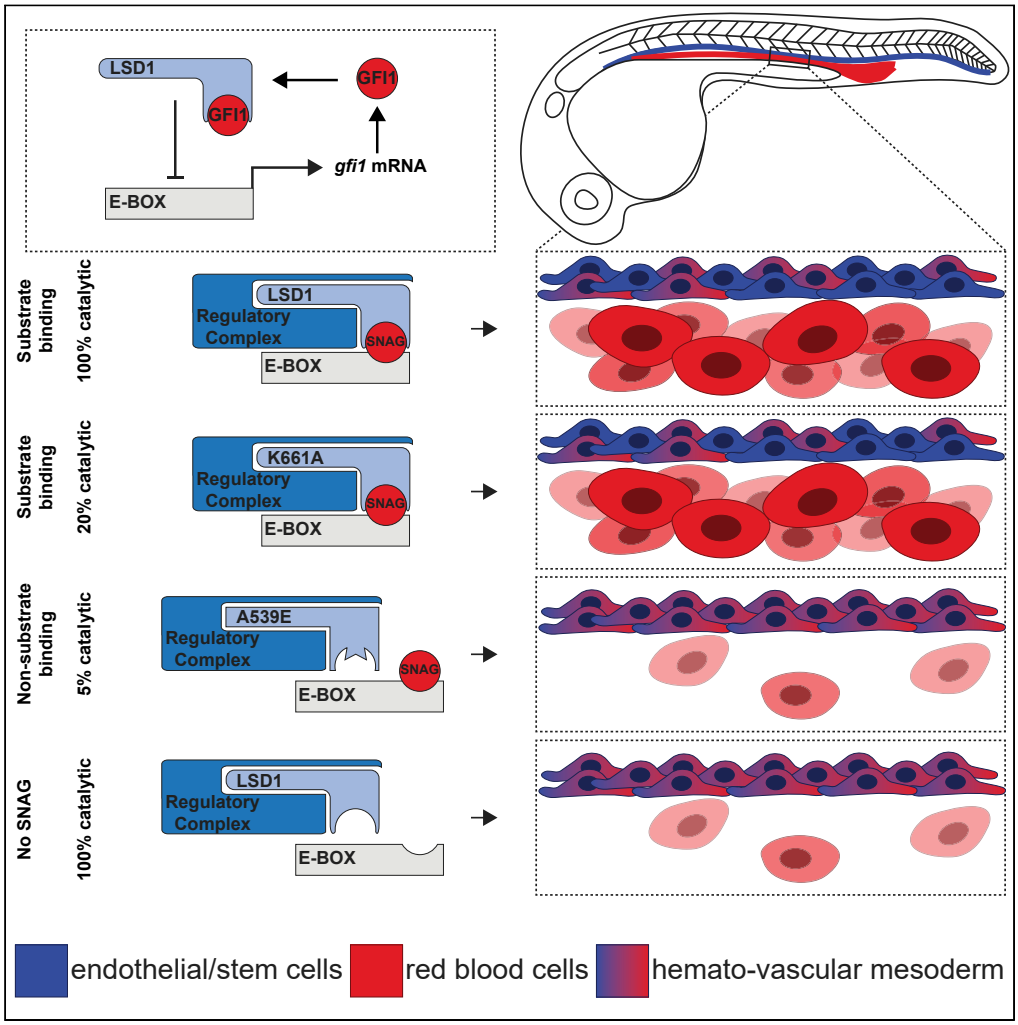

Mattie J. Casey, Alexandra M. Call, Annika V. Thorpe, Cicely A. Jette, Michael E. Engel, Rodney A. Stewart

mee2mj@hscmail.mcc.virginia.edu (M.E.E.)
rodney.stewart@utah.edu (R.A.S.)

Highlights

LSD1 controls embryonic gene expression by a catalysis-independent scaffold function

SNAG-domain binding to LSD1 is critical for its scaffold function

LSD1-GFI1 generates a negative feedback loop to repress *gfi1* expression *in vivo*

Casey et al., iScience *26*, 105737
January 20, 2023
https://doi.org/10.1016/j.isci.2022.105737

iScience

CellPress
OPEN ACCESS

Article

The scaffolding function of LSD1/KDM1A reinforces a negative feedback loop to repress stem cell gene expression during primitive hematopoiesis

Mattie J. Casey,[1] Alexandra M. Call,[1] Annika V. Thorpe,[1] Cicely A. Jette,[1] Michael E. Engel,[2,*] and Rodney A. Stewart[1,3,*]

SUMMARY

Lsd1/Kdm1a functions both as a histone demethylase enzyme and as a scaffold for assembling chromatin modifier and transcription factor complexes to regulate gene expression. The relative contributions of Lsd1's demethylase and scaffolding functions during embryogenesis are not known. Here, we analyze two independent zebrafish *lsd1/kdm1a* mutant lines and show Lsd1 is required to repress primitive hematopoietic stem cell gene expression. Lsd1 rescue constructs containing point mutations that selectively abrogate its demethylase or scaffolding capacity demonstrate the scaffolding function of Lsd1, not its demethylase activity, is required for repression of gene expression *in vivo*. Lsd1's SNAG-binding domain mediates its scaffolding function and reinforces a negative feedback loop to repress the expression of SNAG-domain-containing genes during embryogenesis, including *gfi1* and *snai1/2*. Our findings reveal a model in which the SNAG-binding and scaffolding function of Lsd1, and its associated negative feedback loop, provide transient and reversible regulation of gene expression during hematopoietic development.

INTRODUCTION

Lysine (K)-specific demethylase 1A (LSD1, also known as KDM1A) is a well-established and highly conserved flavin adenine dinucleotide (FAD)-dependent demethylase that controls gene expression during differentiation and development. LSD1 functions through interaction with multiprotein complexes, such as BHC/CoREST (BRAF-histone deacetylase complex/Corepressor for element-1-silencing transcription factor), NuRD (nucleosome remodeling and deacetylase), and CtBP (C-terminal binding protein), to remove mono- and di-methyl marks from histone 3 lysine 4 (H3K4) and histone 3 lysine 9 (H3K9).[1,2] LSD1 also demethylates transcription factors such as TP53 and E2F1 to modulate transcriptional programs.[3–5] Evidence from multiple malignancy models indicates that LSD1 may also have non-catalytic functions.[6–11] For example, in acute myeloid leukemia (AML) cells, LSD1 enzymatic activity is not required for cell survival or differentiation. Instead, LSD1 acts as a scaffold for recruiting the growth factor independence 1 protein (GFI1) to enhancer regions located adjacent to genes that regulate myeloid differentiation and survival.[6,7,9] The relative contribution of LSD1's catalytic and non-catalytic functions during tumorigenesis and normal development, however, are not well understood. Such knowledge will be essential for understanding and manipulating LSD1-dependent gene expression programs for therapeutic purposes.

Hematopoiesis in vertebrates is characterized by two separate developmental programs called the primitive and definitive waves.[12–14] The primitive wave primarily gives rise to early erythrocytes and macrophages in the developing embryo. Immediately following the primitive wave, the definitive wave generates hematopoietic stem cells (HSCs) that differentiate into all blood lineages of the adult organism.[12–14] LSD1 is essential for the development of HSCs and granulocytes, and for erythroid differentiation.[15–20] Germline deletion of *Lsd1* in mice is embryonic lethal by day E6.5, and conditional *Lsd1* deletion in hematopoietic stem cells and erythroid cells causes severe anemia.[17,21,22] Similarly, germline mutations in *lsd1* in zebrafish result in embryonic lethality, failure to generate primitive erythrocytes[19] and loss of expression of essential erythrocyte genes such as *gata1*.[19,20] Of interest, recent studies suggest that the primitive hematopoietic defects in zebrafish *lsd1* mutants are demethylase-independent.[20] However, the basis for assigning a demethylase-independent role for Lsd1 was derived from the use of a presumed catalytically dead *lsd1* rescue

[1]Department of Oncological Sciences, Huntsman Cancer Institute, University of Utah, 2000 Circle of Hope Drive, Salt Lake City, UT 84112, USA

[2]Department of Pediatric Hematology/Oncology, Emily Couric Cancer Center, University of Virginia, Charlottesville, VA 22903, USA

[3]Lead contact

*Correspondence: mee2mj@hscmail.mcc.virginia.edu (M.E.E.), rodney.stewart@utah.edu (R.A.S.)

https://doi.org/10.1016/j.isci.2022.105737

construct,[20] which has subsequently been shown to retain up to 20% normal Lsd1 activity.[23] Thus, a demethylase-independent role for Lsd1 during hematopoietic differentiation remains debatable. More importantly, the mechanism underlying Lsd1's repression of gene expression during primitive hematopoiesis *in vivo* remains unknown.

Both the catalytic and scaffolding functions of LSD1 are thought to require a hydrophobic pocket within the LSD1 protein that enables substrate binding.[24,25] The structure of LSD1 includes an N-terminal amine-oxidase-like domain (AOL), a central tower domain, and a C-terminal AOL domain. The AOL domains fold around the tower domain to form the substrate-binding hydrophobic pocket that contains an FAD cofactor essential for LSD1's catalytic activity.[24,25] The binding of histone tails to the hydrophobic pocket is required for their demethylation by LSD1. The non-catalytic or scaffolding functions of LSD1 appear to be mediated through direct binding to transcription factors that contain a highly conserved, 21-amino-acid, N-terminal domain called the SNAIL/GFI ("SNAG") domain, which resembles the structure of the tail region of histone H3 and binds to the same hydrophobic pocket in LSD1.[26,27]

Transcriptional repression mediated by either GFI- or SNAIL-family proteins is critical for normal embryonic development.[28,29] The SNAIL family of zinc-finger transcription factors direct many cellular processes, including the formation of mesoderm and neural crest cells, and the epithelial-to-mesenchymal transition (EMT) in both development and malignancy.[29] GFI1 and GFI1B are important drivers of both hematopoietic stem cell (HSC) differentiation and leukemogenesis.[18,30,31] GFI1 promotes normal lymphoid and myeloid development whereas GFI1B promotes the generation of erythrocytes and megakaryocytes.[31,32] A common attribute of these SNAG-domain-containing transcription factors is their ability to negatively regulate their own gene expression and that of other members of their gene family.[29,33–39] The SNAG-dependent transcriptional feedback loops as well as the GFI- and SNAIL-mediated developmental programs are dependent on interactions between these transcription factors and LSD1 *in vitro*[26,40]; however, whether such interactions also mediate feedbacks loops during embryogenesis remains unknown.

The mechanistic basis for LSD1-mediated primitive hematopoiesis has not yet been investigated *in vivo*. Here, we performed RNA-Sequencing (RNA-Seq) to analyze the transcriptional program regulated by Lsd1 during primitive hematopoiesis using two previously undescribed *lsd1* zebrafish mutants. Surprisingly, only a limited number of genes were upregulated in *lsd1* mutants and were enriched for *snail1/2* and *gfi* family genes, suggesting that Lsd1 normally functions to selectively repress SNAG-domain-containing genes during embryogenesis. As expected,[20] we found that loss of *lsd1* impaired erythrocyte development *in vivo* and that both wild-type Lsd1 and the Lsd1-K661A catalytic mutant rescued defective primitive hematopoiesis in *lsd1*-mutant embryos. Therefore, to determine whether Lsd1 binding to SNAG-domain-containing proteins is needed for Lsd1-mediated hematopoiesis, we analyzed the structure of SNAG-domain-bound Lsd1 and mutated amino acid residues that were likely critical for Lsd1 binding to SNAG-domain-containing proteins but not its catalyic activity. None of these SNAG-binding-compromised Lsd1 mutant proteins were able to rescue defective hematopoiesis in the *lsd1* mutants. Moreover, injection of embryos with an exogenous SNAG peptide inhibited the ability of wild-type Lsd1 to rescue defective hematopoiesis in the *lsd1* mutants. These experiments show that LSD1 controls gene expression during primitive hematopoiesis primarily via its scaffolding function, which requires binding to SNAG-domain-containing proteins. In addition, we demonstrate that SNAG-dependent binding to LSD1 represses the expression of SNAG-containing genes themselves, thereby reinforcing a negative feedback loop to control gene expression during embryogenesis.

RESULTS

Newly identified zebrafish *lsd1* alleles confirm that Lsd1 function is required for erythrocyte development *in vivo*

The zebrafish genome contains one copy of the *lsd1* gene, which encodes for a protein that is highly identical (>90%) to human *LSD1* (Figure 1A). Zebrafish *lsd1* was previously analyzed using a mutant allele, *lsd1*^{it627}, that was identified through an N-ethyl-N-nitrosourea (ENU) mutagenesis screen and found to contain a premature stop codon (replacing Gln609) that leads to a truncation of the Lsd1 protein within the C-terminal amine-oxidase-like (AOL) domain[19]. This mutation was reported to promote endothelial cell differentiation at the expense of erythroid cell development as early as 12.5 h post-fertilization (hpf), and to cause lethality by 10 days post-fertilization (dpf).[19] To verify that Lsd1 is required for erythroid

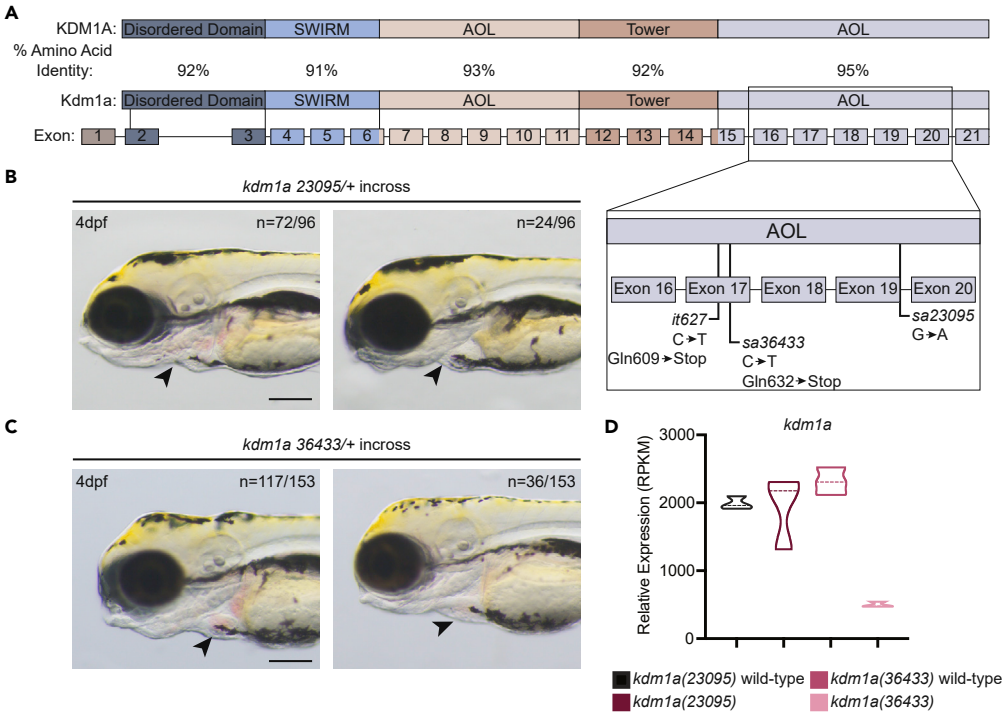

Figure 1. Mutant *lsd1* alleles in zebrafish

(A) Schematic showing the percent amino acid identity between human and zebrafish Lsd1 as well as the locations of the mutations in the C-terminal AOL region that are relevant to this study.

(B and C) Brightfield images of 4-dpf embryos derived from an incross between either *kdm1a(23095)* heterozygotes (B) or *kdm1a(36433)* heterozygotes (C). Arrowheads indicate erythrocytes in the heart. The number of animals with a similar phenotype to the representative image, out of the total number of animals visualized, is shown in the top right to indicate Mendelian ratio. Scale bar, 200 μm.

(D) The relative mRNA expression levels of *kdm1a* in mutants and wild-type siblings are shown in the graph.

cell development in zebrafish, we analyzed two previously uncharacterized ENU-generated *lsd1* alleles called *kdm1a(sa23095)* and *kdm1a(sa36433)*. The *kdm1a(23095)* allele contains a donor-splice-site mutation at the C-terminus of exon 19, and *kdm1a(36433)* contains a premature stop mutation in exon 17 that replaces Gln632 (Figure 1A).[41] Zebrafish that are homozygous mutant for either allele fail to survive to adulthood. Embryos derived from an incross between either *kdm1a(23095)* or *kdm1a(36433)* were grown to 4 dpf, and the developing cardiac region was examined for red cells (erythrocytes). Consistent with *lsd1*^{it627} mutants, a quarter of the embryos derived from either incross exhibited a lack of red cells, suggesting that *kdm1a(23095)* and *kdm1a(36433)* homozygous mutants either fail to generate erythrocytes or their erythrocytes have a reduction or loss of hemoglobin (known as "pale erythrocytes", Figures 1B and 1C). To better understand the effect of the *kdm1a(23095)* and *kdm1a(36433)* mutations on their respective mRNA expression levels, we performed RNA-Seq and found that *lsd1* mRNA levels were similar between *kdm1a(23095)* mutants and their wild-type siblings, whereas *kdm1a(36433)* mRNA was largely undetectable, indicating that it is likely degraded through nonsense-mediated decay (Figure 1D). Examination of the mutant *kdm1a(23095)* allele with the Integrative Genomics Viewer revealed that it leads to *lsd1* mRNA transcripts containing either an excision of exon 19 or a retention of the intron between exon 19 and 20 (Figure S1A). Both scenarios are predicted to produce a non-functional protein because they would disrupt the C-terminal AOL domain, which is critical for forming the substrate- and FAD-binding subdomains. Finally, to determine if the *kdm1a(23095)* and *kdm1a(36433)* mutations disrupt hematopoietic gene expression programs during primitive hematopoiesis similar to the *lsd1*^{it627} mutants,[19] we analyzed the expression of erythrocyte (*gata1*) and endothelial-cell (*etv2* and *fli1a*) markers by whole-mount *in situ* hybridization (WISH). Indeed, *kdm1a(23095)* and *kdm1a(36433)* homozygous mutants showed diminished *gata1* expression (Figures S1B and S1E) and elevated *fli1a* (Figures S1C and S1F) and *etv2* (Figures S1D and S1G) expression. The reduction in primitive erythrocytes did not appear to be driven by an overall increase in apoptotic cells or decrease in cellular proliferation in the tail region encompassing the

intermediate cell mass (ICM), because there were no significant changes in activated-Caspase-3-positive cells or phospho-histone-H3-positive cells, respectively, in *lsd1* mutants in this region (see Figure S2 and STAR Methods). Thus, a phenotypic analysis of three different zebrafish *lsd1* mutant alleles from two different laboratories demonstrates highly reproducible and robust primitive hematopoietic defects *in vivo* that support a model in which loss of LSD1 function is required for the differentiation of primitive hematopoietic cell types, such as erythrocytes, during embryonic development.

gfi1 hematopoietic transcriptional regulators are de-repressed in *lsd1* mutants

We next questioned whether the *lsd1*-mutant primitive hematopoietic phenotypes were because of a block in differentiation via mis-regulation of hematopoietic stem cell transcription factors. The GFI family of transcription factors, GFI1 and GFI1B, were likely candidates because they both require LSD1 to mediate gene repression for lineage-specific differentiation in hematopoiesis.[6,9,18,40] Both GFI1 and GFI1B can autoregulate as well as cross-regulate expression from their respective genes to modulate hematopoietic-lineage differentiation.[33–37] This autoregulation is dependent on functional SNAG and DNA-binding domains within the GFI1 and GFI1B proteins.[26,33,34,36,42] The zebrafish genome contains three *gfi* family members. The *gfi1aa* and *gfi1ab* genes are homologous to human *GFI1*, whereas *gfi1b* is homologous to human *GFI1B*.[43] We performed WISH in 24-hpf *lsd1* mutants and siblings and found that *gfi1aa* expression is normally observed exclusively in the ICM and is upregulated in *lsd1* mutants (Figures 2A and 2D). Expression of the *gfi1ab* gene is normally restricted to hair cells of the developing ear at 24 hpf[44] (Figures 2B and 2E); however, in *lsd1* mutants *gfi1ab* expression is ectopically induced in the anterior lateral plate mesoderm by 14 hpf (Figures S3A and S3B), as well as the ICM at 24 hpf (Figures 2B and 2E), and remains elevated in the caudal hematopoietic tissue (CHT) at 3 dpf (Figure S3C). The *gfi1b* gene is normally expressed in the ICM at 24 hpf, and WISH analysis showed no qualitative difference in *gfi1b* ICM expression between *lsd1* mutants and siblings at this stage (Figures 2C and 2F). However, analysis of *gfi1b* expression by WISH at 3 dpf showed elevated *gfi1b* in the CHT (Figure S3D). These data indicate that Lsd1 is required to repress *gfi1* paralog expression during zebrafish primitive hematopoiesis.

Genetic mutants in *gfi1/1b* phenocopy *lsd1* mutant hematopoietic defects

Gfi1/1b family members control the differentiation of stem/progenitor cells into different lineages during hematopoiesis,[18,30,31] in part through repressing their own expression during lineage commitment.[33–37] Our WISH analysis of *gfi1/1b* genes in *lsd1* mutants suggested that Lsd1 is required for Gfi1 and Gfi1b to repress their own expression *in vivo*, particularly *gfi1ab*. Thus, we next hypothesized that the loss of differentiated hematopoietic cell types in *lsd1* mutants is because of loss of Gfi1/1b function. To test this possibility, we analyzed primitive hematopoiesis in *gfi1aa; gfi1ab; gfi1b* triple mutants (Figure S4). We found that loss of *gfi1/1b* genes in zebrafish caused loss of primitive hematopoietic markers, including *gata1* expression at 24 hpf in the ICM (Figure S4B) as well as other morphological abnormalities (Figure S4C). Indeed, during the course of this study, another group reported similar results with *gfi1/1b* triple mutants.[45] We also analyzed individual mutants in the Gfi1 family and found that, similar to Wu et al.,[45] loss of *gfi1aa* is largely sufficient to phenocopy the *lsd1* mutant hematopoietic phenotypes, with a minor contribution by loss of *gfi1ab* (data not shown). Together, these studies support a model in which Lsd1 is required for Gfi1aa to repress the expression of itself and other family members, particularly *gfi1ab*, which in turn is required for the generation of differentiated primitive hematopoietic cell types, such as *gata1*-expressing erythrocytes.

Lsd1 broadly regulates the mRNA expression of SNAG domain transcription factors

As a histone demethylase, LSD1 is predicted to impact the expression of multiple genes during embryogenesis, mainly through transcriptional repression by demethylation of H3K4. To better understand how LSD1 controls gene expression during embryogenesis, we used a scalpel to cut 24-hpf embryos derived from an incross of kdm1a(23095) or kdm1a(36433) heterozygotes just posterior to the yolk sac (Figure 3A). The head was used to genotype the embryo and the tail was preserved in RNA stabilization solution. On completion of genotyping, five tails from homozygous *lsd1* mutants or wild-type siblings were pooled, and RNA-Seq was performed on the pooled RNA (Figure 3B, Table S4). Despite Lsd1's established role as an epigenetic modifier, we found that the expression of only a small subset of genes was significantly affected by loss of *lsd1* at this stage of embryogenesis. Of 21,497 genes, 409 were upregulated and 524 were downregulated ($p<0.05$, Figure 3B, Table S4). Examination of the most differentially expressed genes in *lsd1* mutants revealed three important findings: (1) An enrichment among the upregulated genes for

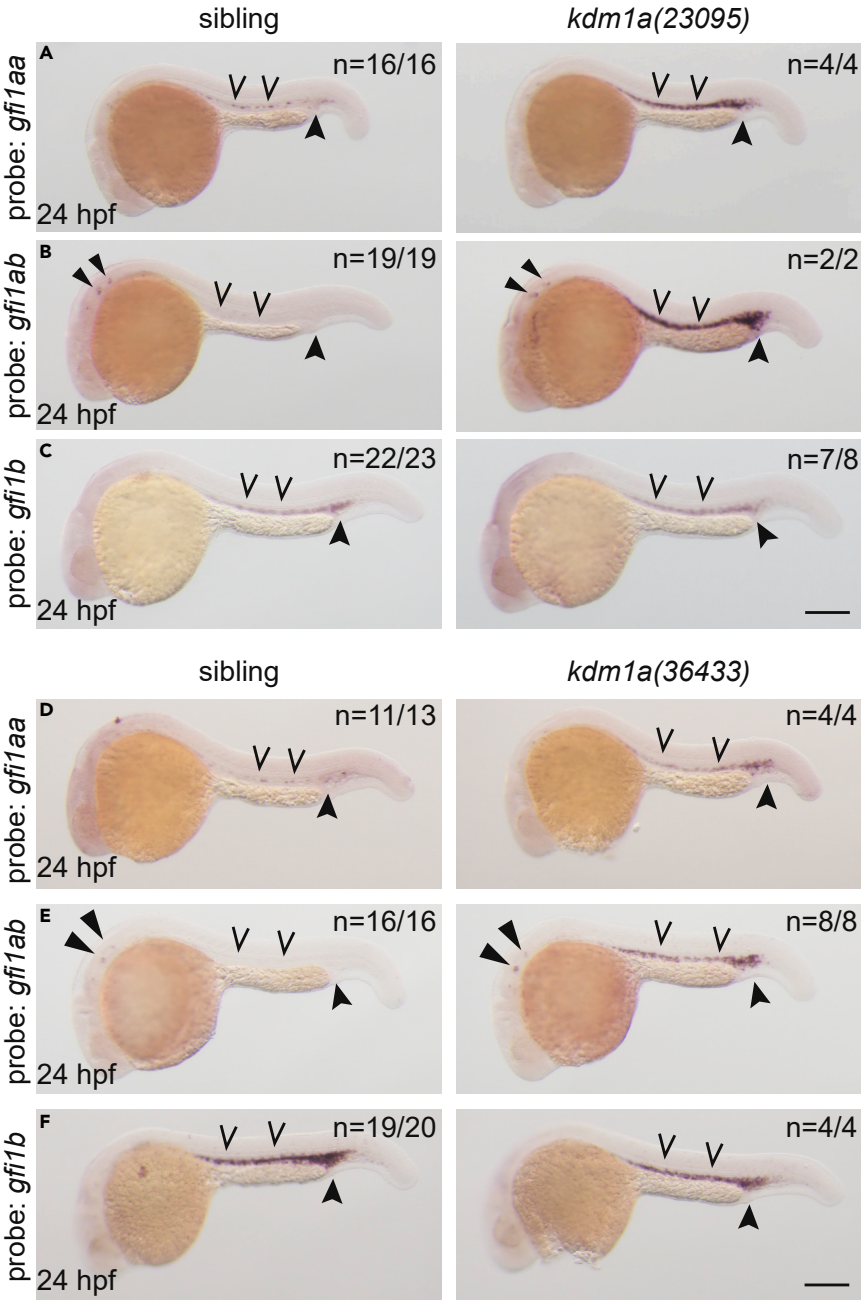

Figure 2. Expression of GFI-family transcription factors are dysregulated in *lsd1* mutants

(A–F) Whole-mount *in situ* hybridization (WISH) of embryos derived from an incross of either *kdm1a(23095)* heterozygotes (A–C) or *kdm1a(36433)* heterozygotes (D–F) using probes to detect *gfi1aa* (A and D), *gfi1ab* (B and E), or *gfi1b* (C and F), as indicated. Representative images are shown with the number of animals with similar staining patterns for the indicated genotype shown in the upper right corner of each image. The lower left corner indicates the approximate stage of the animal at the time of fixation. Embryos were imaged, blindly scored by expression levels and then genotyped by HRMA. Carons indicate ICM expression; closed arrowheads indicate posterior blood island/caudal hematopoietic tissue; narrow triangles indicate inner-hair-cell expression. Scale bar, 200 μm.

SNAG-domain-containing transcription factors (Figure 3B), including both *gfi* and *snail* family genes, (2) elevated levels of endothelial/hematopoietic stem or progenitor genes, including *tbx16*, *etv2*, *lmo2*, *gfi1aa* and *tal1* (Figure S5), and (3) decreased levels of differentiated hematopoietic cell markers, such as *lyz* and *hbbe1.3* (Figure S5). These findings were consistent with the WISH analysis above showing differential

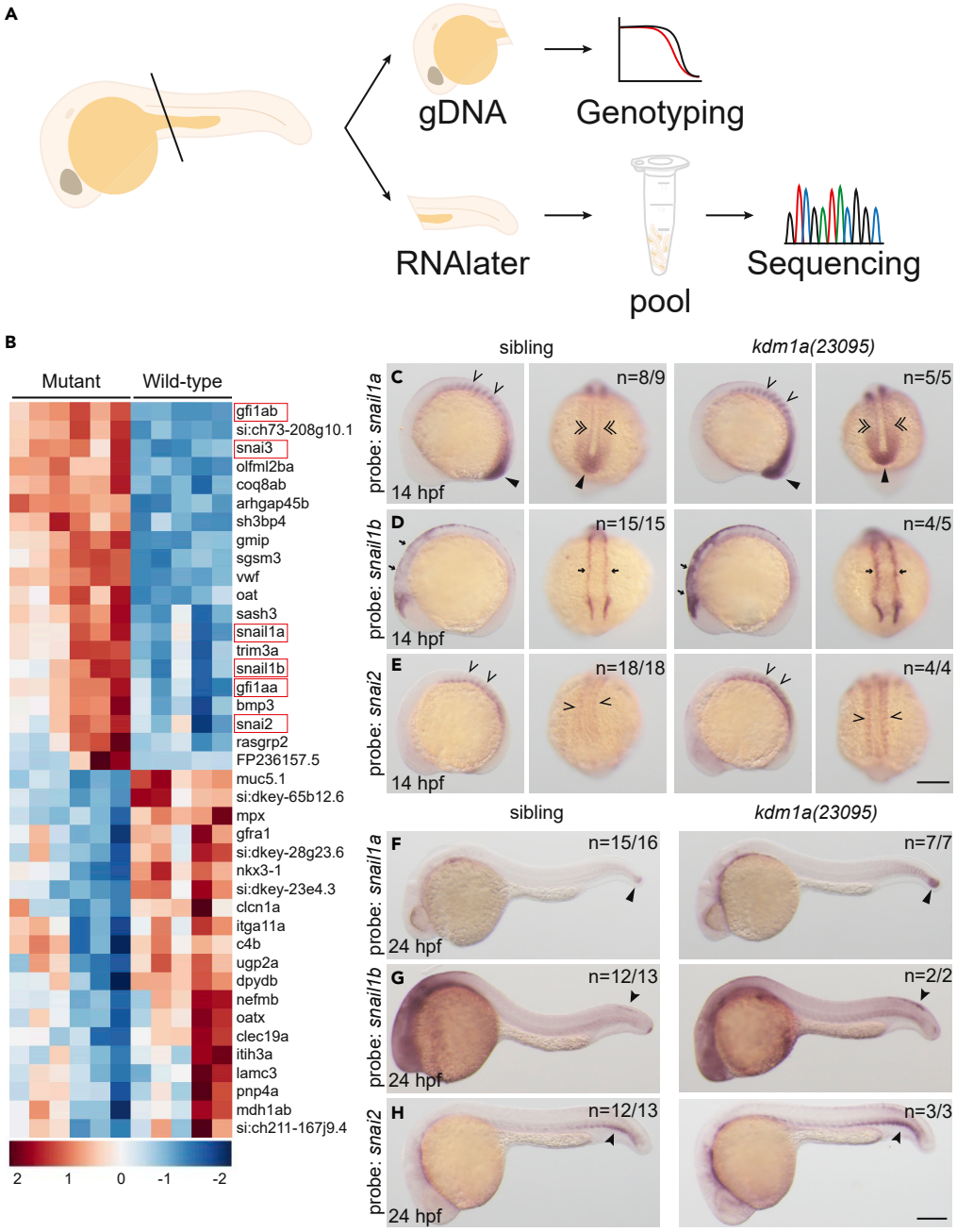

Figure 3. SNAG-domain proteins are dysregulated in *lsd1* mutants

(A) Schematic of the sample preparation workflow.

(B) Heatmap of the top 40 differentially expressed genes in *kdm1a(23095)* and *kdm1a(36433)* mutants compared to wild-type siblings. SNAG-domain proteins are boxed.

(C–H) WISH of embryos from an incross of *kdm1a(23095)* heterozygotes for *snail1a*, *snail1b*, and *snail2* at 14 hpf (C–E), lateral (left) and dorsal (right) views) and 24 hpf (F–H). Representative images are shown with the number of animals with similar staining patterns for the indicated genotype shown in the upper right corner of each image. The lower left corner indicates the approximate stage of the animal at the time of fixation. Embryos were imaged, blindly scored by expression and then genotyped by HRMA. Carons indicate somite expression; narrow triangles indicate tail bud; double carons indicate adaxial cell expression; arrows indicate neural plate border; closed arrowheads indicate trunk neural crest cells (*snail1b*) or ventral mesoderm (*snai2*). Scale bar, 200 μm.

effects on *gfi1* and *gata1* gene expression in *lsd1* mutants. In addition, they show Lsd1 is normally required to repress hematopoietic/endothelial stem cell genes during embryogenesis, including all *gfi1/1b* genes.

The RNA-Seq analysis suggests that Lsd1 function is required to regulate a limited number of genes during early embryogenesis, and that SNAG-domain-containing genes as a group are targeted by Lsd1 for repression. To determine the extent to which Lsd1 is required to repress the expression of SNAG-domain-containing genes in other embryonic tissues, WISH experiments were performed on embryos from a *lsd1*-heterozygous mutant incross at 14 and 24 hpf (Figures 3C–3H). We observed the upregulation of *snail1a*, *snail1b* and *snai2* in a number of different cell types, including muscle, lateral plate mesoderm, neural crest and tailbud. These data show that LSD1 functions in a number of embryonic tissues to selectively repress the expression of SNAG-domain-containing genes.

Wild-type Lsd1 restores normal expression levels of primitive hematopoietic transcription factors in *lsd1* mutants

To determine if expression of *lsd1* mRNA can repress expression of *gfi1aa* and *gfi1ab* in *kdm1a(23095)* and *kdm1a(36433)* mutants, we injected embryos derived from a heterozygous in-cross of each mutant line with mRNA encoding either wild-type zebrafish *lsd1* (*zlsd1*) or human *LSD1* (*hLSD1*). We then confirmed the level of protein expression via western blot (Figure S6) and performed WISH. Indeed, the injection of either wild-type *zlsd1* mRNA or wild-type *hLSD1* mRNA was sufficient to repress *gfi1aa* and *gfi1ab* expression, and to restore *gata1* expression, in both *kdm1a(23095)* and *kdm1a(36433)* embryos (Figures 4A–4F and S7A–S7F). Moreover, the injection of mRNA encoding *zlsd1-ΔQ632*, which mimics the predicted *kdm1a(36433)* protein product (a premature stop codon substituted at Gln632), and mRNA encoding *lsd1* lacking the C-terminal AOL domain failed to rescue changes in the transcriptional program (Figures S8 and S9). Although our data is consistent with previous reports showing conservation of Lsd1 function with respect to restoring *gata1* expression,[20] it shows that the ability of LSD1 to repress expression of *gfi1aa/ab* genes during primitive hematopoiesis is also conserved. As Lsd1 is largely associated with the repression of gene expression, such findings allowed us to design assays to interrogate the mechanism(s) required for Lsd1's repressive function *in vivo*.

Lsd1 variants that impair catalytic activity have differential effects on restoring gene expression during primitive hematopoiesis

LSD1 catalytic activity occurs through an FAD cofactor intermediate.[24,25] In the LSD1 hydrophobic pocket, the H3K4 residue from the bound histone H3 tail is located in close proximity to the N5 atom of FAD,[46] which enables FAD to oxidize the methylated lysine. This converts the methylated lysine to an intermediate imine molecule and a demethylated side chain.[47] The imine is then hydrolyzed to formaldehyde, and the flavin cofactor is reoxidized by molecular oxygen to complete the enzymatic cycle.[47] Several residues are required for LSD1 demethylase activity on *in vitro* substrates such as dimethylated histone H3 peptides or reconstituted nucleosomes.[23–25] In general, there are two groups of mutations that impair LSD1 catalytic activity on histone substrates: (1) Mutations that interfere with stabilization and subsequent oxidization of the reduced flavin, such as the LSD1 K661A allele and (2) mutations located in the hydrophobic pocket that are required for the binding of LSD1 to the histone H3 tail, such as the LSD1 A539E allele.[23,25,27] Notably, because the LSD1 K661A allele does not demethylate histone peptides, it has been widely used to infer catalysis-independent functions of LSD1 in different cell- and animal-based processes, including zebrafish primitive hematopoiesis.[20] However, recent studies showed that the LSD1 K661A allele retains approximately 20% of its wild-type histone demethylase activity when combined with reconstituted nucleosome substrates.[23] In contrast, the demethylase activity of the LSD1 A539E allele is significantly impaired using both peptide and nucleosome substrates, retaining only ~5% of wild-type LSD1 activity. We therefore determined the extent to which these catalytically impaired LSD1 mutations could restore primitive hematopoietic gene expression programs *in vivo*. Similar to wild-type *zlsd1* mRNA, injection of $zlsd1^{K661A}$ mRNA into both *kdm1a(23095)* and *kdm1a(36433)* mutants rescued normal expression patterns of *gfi1ab* and *gata1* expression during primitive hematopoiesis (Figures 5 and S10).[20] In contrast, injection of mRNA encoding $zlsd1^{A539E}$ failed to repress *gfi1ab* expression or restore *gata1* levels (Figures S11A and S11B) despite robust Lsd1 A539E protein expression (Figure S6). These data show that catalytically impaired Lsd1 alleles have differential outcomes with respect to rescue of gene expression programs, revealing that either a threshold level of LSD1 nucleosome-based catalytic activity (between 5 and 20%), or integrity of the substrate binding domain of LSD1, or both, are required to control gene expression programs during primitive hematopoiesis *in vivo*.

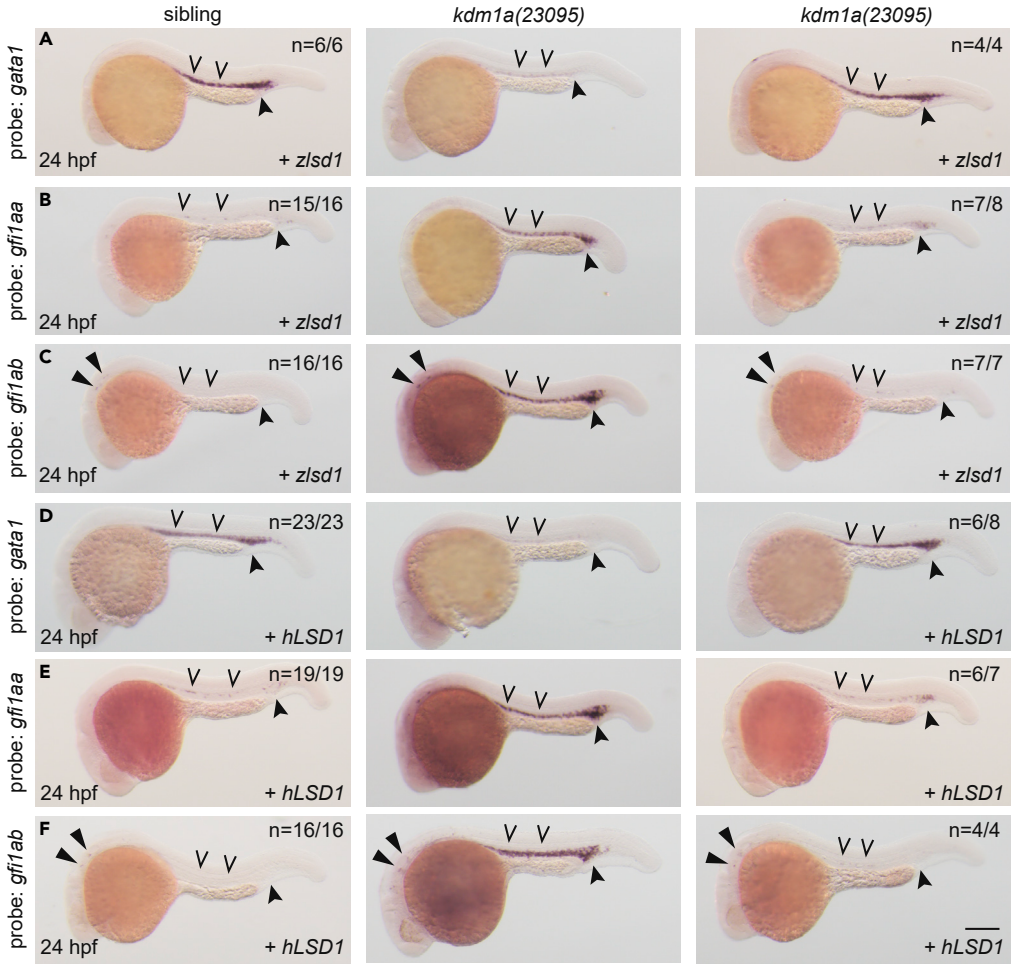

Figure 4. Wild-type *lsd1* rescues hematopoietic transcription factor expression

(A–F) Single-cell embryos from a *kdm1a(23095)* heterozygous incross were injected with either *zlsd1* (A–C) or *hLSD1* mRNA (D–F). At 24 hpf, WISH was performed. Representative images are shown with the number of animals with similar staining patterns for the indicated genotype shown in the upper right corner. The lower right corner indicates the mRNA injection conditions. Uninjected mutant embryos are shown in the middle column for comparison. Embryos were imaged, blindly scored by expression and then genotyped by HRMA. Carons indicate ICM expression; closed arrowheads indicate posterior blood island/caudal hematopoietic tissue; narrow triangles indicate inner-hair-cell expression. Scale bar, 200 μm.

SNAG-domain binding to Lsd1 is required for Lsd1-mediated regulation of primitive hematopoiesis

To determine whether SNAG-domain binding is specifically required for LSD1-mediated transcription during primitive hematopoiesis, we sought to design SNAG-binding mutations in LSD1. We analyzed the crystal structure of LSD1 in complex with an N-terminal SNAIL SNAG peptide[27] and identified LSD1 residues in the hydrophobic pocket that were within 4 Å of the first six amino acids of the peptide (Table S1). To interfere with SNAG-dependent binding of Lsd1 without significantly impacting its FAD-dependent catalytic activity, we chose to analyze the Asp555 residue, which is conserved from humans to zebrafish (D555, Figure 6A) and located within 4 Å of the proline-2 residue of the SNAG domain that is essential for its binding to LSD1 (Figure 6B, top panel).[40,42] We mutated the negatively charged Asp555 to a positively charged Lys (D555K, Figure 6B, bottom panel). We found that, similar to injection of substrate-binding-mutant *zlsd1*^{A539E} mRNA, injection of *zlsd1*^{D555K} mRNA into *lsd1* mutants was unable to restore *gata1* (Figure 6C) or repress *gfi1ab* (Figure 6D) gene expression. As the LSD1 D555K mutant protein retains more LSD1 demethylase activity than the LSD1 K661A mutant protein on histone peptides,[24,25] our data supports a model in which LSD1's regulation of primitive hematopoietic gene expression programs is largely catalysis-independent.

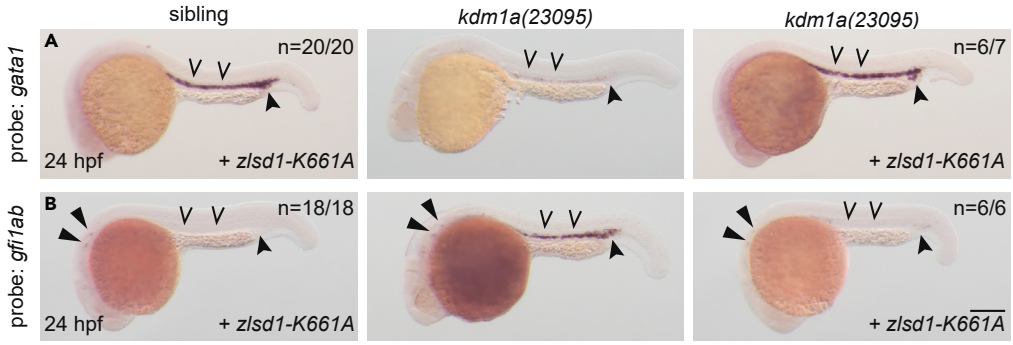

Figure 5. Demethylase-deficient *lsd1* rescues hematopoietic transcription factor gene expression

(A and B) Single-cell zebrafish embryos from a *kdm1a(23095)* heterozygous incross were injected with zebrafish *zlsd1-K661A*. WISH was then performed at 24 hpf for *gata1* (A) and *gfi1ab* (B). Representative images are shown with the number of animals with similar staining patterns for the indicated genotype shown in the upper right corner. The lower right corner indicates the mRNA injection conditions. Uninjected mutant embryos are shown in the middle column for comparison. Embryos were imaged, blindly scored by expression and then genotyped by HRMA. Carons indicate ICM expression; closed arrowheads indicate posterior blood island/caudal hematopoietic tissue; narrow triangles indicate inner-hair-cell expression. Scale bar, 200 μm.

To our knowledge, the LSD1 K661A mutation represents the most well-characterized catalytically-impaired molecule that does not interfere with substrate binding.[23–25] Mutations at other LSD1 residues, such as D555 and A539, have been shown both to impair catalytic activity and interfere with substrate binding,[23–25] and we found no published LSD1 mutants that block substrate binding without also negatively impacting LSD1 catalytic activity. Therefore, to test whether blocking substrate binding to LSD1 is sufficient to disrupt gene expression *in vivo*, we synthesized a peptide representing the SNAG domain (Figure 7A), which we and others have previously shown to bind to LSD1 *in vitro*.[6,26,27,48,49] We injected the SNAG-domain peptide with wild-type *lsd1* mRNA into one-cell-stage zebrafish embryos derived from an incross between heterozygous *lsd1* mutants and analyzed *gata1* and *gfi1ab* expression by WISH. We found that the SNAG-domain peptides blocked the ability of wild-type Lsd1 to both restore normal *gata1* expression and repress *gfi1ab* expression in *lsd1* mutants (Figures 7B and 7C). These data further support a model in which LSD1's regulation of gene expression during primitive hematopoiesis *in vivo* relies primarily on scaffolding and SNAG-domain transcription factor binding, rather than its demethylase activity.

The Lsd1 tower domain is required for Lsd1-mediated regulation of primitive hematopoiesis

Once LSD1 is recruited by SNAG-domain-containing transcription factors to specific genomic locations, it can form a variety of different multiprotein complexes, including BHC/CoREST, NuRD, and CtBP, to regulate gene transcription.[1,5,50] The tower domain of LSD1 is its most well-established protein-protein interaction domain and is critical for binding RCOR1, MTA1, MTA2, and SIN3A.[24,50,51] To determine whether the SNAG-dependent function of Lsd1 requires the tower domain for multiprotein-complex recruitment and subsequent transcriptional regulation, we injected mRNA encoding a zebrafish *lsd1* allele with deletion of the tower domain (*zlsd1-ΔTower*) into embryos derived from an incross between *kdm1a(23095)* heterozygotes and examined gene expression by WISH. Indeed, the *zlsd1-ΔTower* mRNA was unable to restore normal *gata1* or *gfi1ab* expression (Figures 7D and 7E), showing that the LSD1 scaffolding function is critical for LSD1-mediated transcriptional regulation during primitive hematopoiesis.

We propose a model in which the SNAG domains of SNAG-domain-containing proteins recruit LSD1, which acts as a scaffold to assemble chromatin-modifying complexes (such as BHC/CoREST) to repress early developmental programs (such as primitive hematopoiesis, Figure 7F, panel I). In the absence of LSD1, repressive complexes are not recruited to SNAG-bound targets, preventing the down-regulation of endothelial/hematopoietic stem cell programs required to initiate primitive myeloid and erythroid differentiation (Figure 7F, panel II). A catalytically impaired form of LSD1 (K661A) is still able to bind SNAG-domain proteins and repress target genes (Figure 7F, panel III); however, SNAG-binding-impaired LSD1 proteins (e.g., D555K) are unable to repress gene expression (Figure 7F, panel IV). As *gfi1/1b* genes are themselves a target of the LSD1-GFI repressive complex, the scaffolding function of LSD1 also controls a negative feedback loop with GFI1/1B. Thus, the LSD1-GFI1 complex would repress stem and/or

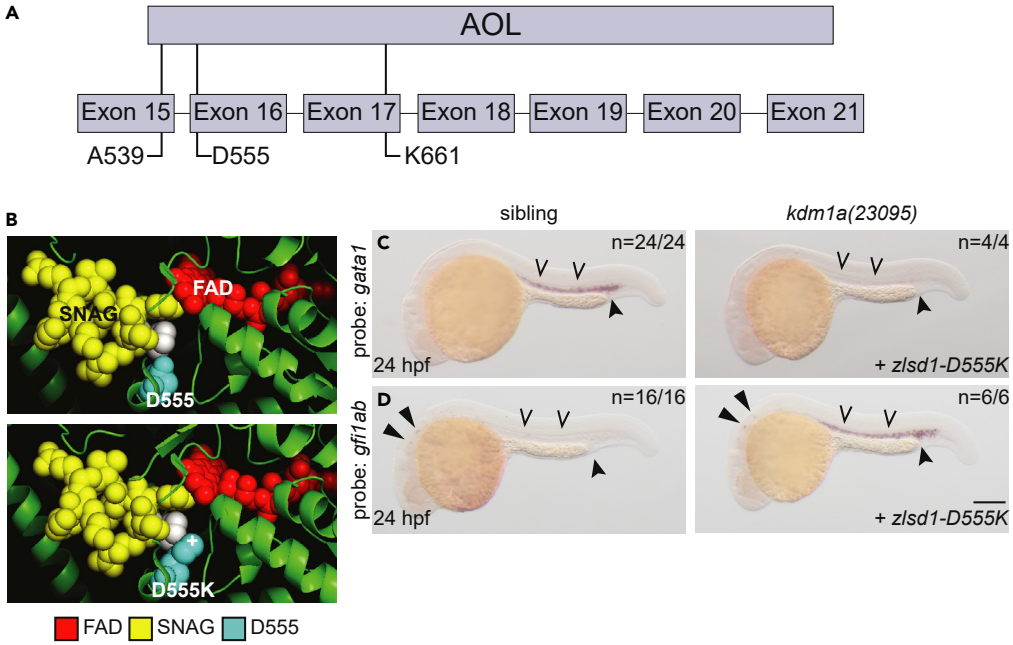

Figure 6. SNAG-binding-deficient *lsd1* does not rescue gene expression

(A) Schematic of the zebrafish Lsd1 C-terminal AOL domain with exon locations of predicted SNAG-binding-deficient mutations indicated.

(B) Top panel: the structure of LSD1 (green) with the FAD moiety (red) and the SNAG domain of SNAIL (yellow) is shown. LSD1 D555 is highlighted in teal. The second proline residue of the SNAG domain is highlighted in white to provide orientation. Bottom panel: the PyMOL mutagenesis feature (PyMOL Molecular Graphics System, Version 2.3.4 Schrodinger, LLC) was utilized to change Asp 555 to Lys. The atom providing positive charge is indicated with a (+) symbol.

(C and D) Single-cell zebrafish embryos from a *kdm1a(23095)* heterozygous incross were injected with mRNA encoding *zlsd1-D555K* (C and D). WISH was then performed on 24-hpf embryos for *gata1* (C) and *gfi1ab* (D) expression. Representative images are shown with the number of animals with similar staining patterns for the indicated genotype shown in the upper right corner. The lower right corner indicates the mRNA injection conditions. Embryos were imaged, blindly scored by expression and then genotyped by HRMA. Carons indicate ICM expression; closed arrowheads indicate posterior blood island/caudal hematopoietic tissue; narrow triangles indicate inner-hair-cell expression. Scale bar, 200 μm.

endothelial genes to promote the initial wave of primitive hematopoietic differentiation, however the subsequent down-regulation of LSD1 scaffold function (through repression of Gfi1/Gfi1b levels) would re-establish the hematopoietic stem cell program to drive definitive hematopoiesis. The catalysis-independent function of LSD1 therefore creates a dynamic system that allows for reversible control of gene expression programs in a progenitor population at different developmental time points, and obviates the need for the reversal of epigenetic/histone events to mediate hematopoietic program switching.

DISCUSSION

LSD1 regulates a diverse array of biological processes through both catalytic and non-catalytic mechanisms that involve interactions with a wide variety of transcription factors and multiprotein complexes. Thus, the inherent complexity of LSD1-mediated gene regulation presents a significant challenge to understanding how LSD1 orchestrates distinct biological outcomes. In this study, we sought to understand the mechanism driving LSD1-mediated transcriptional regulation during primitive hematopoiesis. The catalytically impaired LSD1 K661A mutant protein has been used in a number of studies to identify potential non-catalytic functions both *in vitro* and *in vivo*.[6–11,20] For example, a recent study concluded that LSD1 drives primitive hematopoiesis in a demethylase-independent manner because *zlsd1*^{K661A} was able to restore primitive hematopoiesis in *lsd1*-mutant zebrafish.[20] However, it was subsequently shown that the LSD1 K661A mutant protein retains 20% of its catalytic activity in nucleosome assays.[23] In light of this data, no conclusions can yet be made about whether LSD1's catalytic activity is required for primitive hematopoiesis. Moreover, because all previous reports using *lsd1*-mutant alleles have proven capable of rescuing primitive hematopoiesis in *lsd1*-mutant zebrafish, the domains within LSD1 that are required for LSD1-mediated

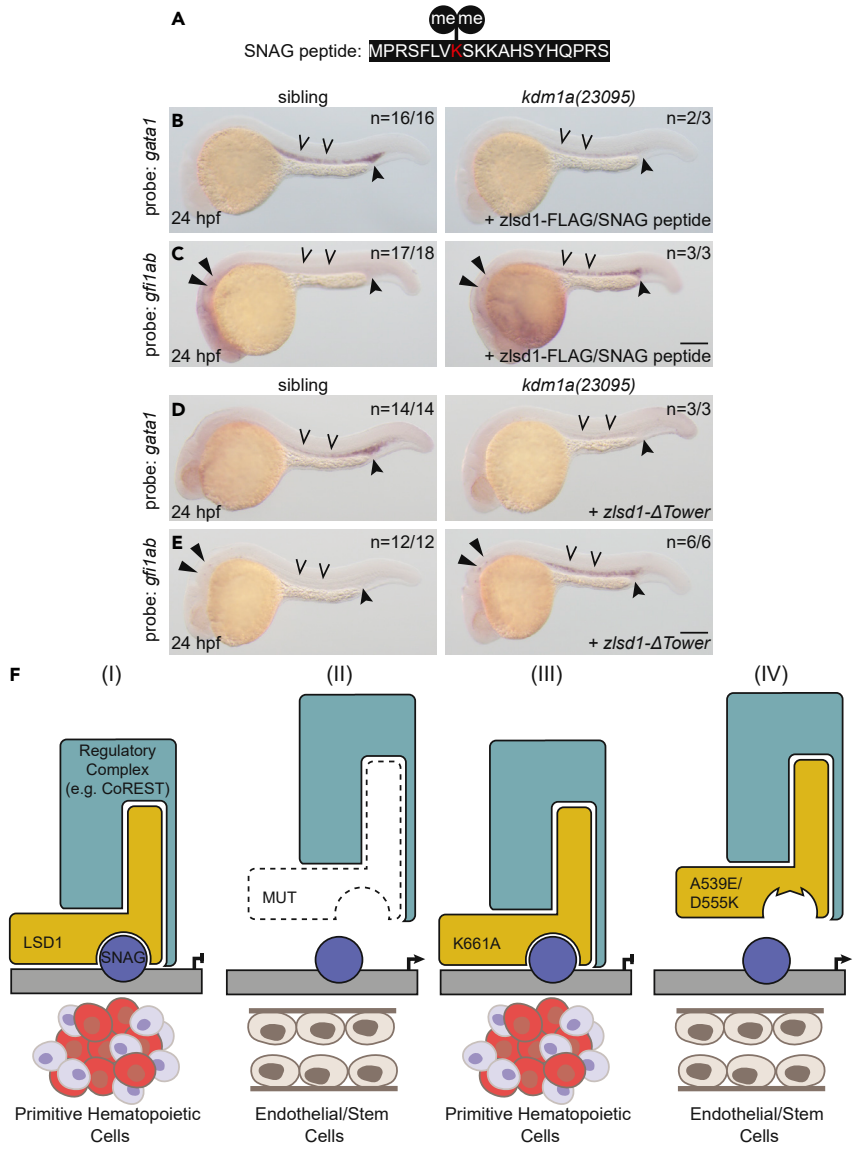

Figure 7. The SNAG-LSD1 interaction is critical for the regulation of primitive hematopoiesis

(A) Sequence of the SNAG domain peptide with dimethylated Lys 8 indicated in red.

(B and C) Single-cell zebrafish embryos from a *kdm1a(23095)* heterozygous incross were injected with both *zlsd1-3XFLAG* mRNA and the SNAG peptide. WISH was then performed at 24 hpf for *gata1* (B) and *gfi1ab* (C) expression.

(D and E) Single-cell zebrafish embryos from a *kdm1a(23095)* heterozygous incross were injected with *zlsd1-ΔTower* mRNA. WISH was then performed at 24 hpf for *gata1* (D) and *gfi1ab* (E) expression. Representative images are shown with the number of animals with similar staining patterns for the indicated genotype shown in the upper right corner. The lower right corner indicates the mRNA injection conditions. Embryos were imaged, blindly scored by expression and then genotyped by HRMA. Carons indicate ICM expression; closed arrowheads indicate posterior blood island/caudal hematopoietic tissue; narrow triangles indicate inner-hair-cell expression. Scale bar, 200 μm.

(F) Model: LSD1-dependent hematopoietic phenotypes require SNAG-domain binding. Under normal conditions, a SNAG-domain protein recruits LSD1 and a regulatory complex (e.g., CoREST) to target specific loci to silence the endothelial/stem program and promote hematopoietic cell differentiation. (II) In the absence of LSD1, SNAG-target loci are not transcriptionally repressed and an endothelial/stem cell fate is permitted. (III) An SNAG-domain protein is still able to recruit a demethylase-deficient LSD1 (K661A) and a regulatory complex to target the genetic loci that enable primitive hematopoietic gene expression. (IV) LSD1 SNAG-domain-binding mutations, such as A539E or D555K, prevent LSD1 from binding SNAG-domain-containing proteins. These LSD1 mutants are therefore not recruited to SNAG-protein target genes, such as endothelial/stem genes, which remain expressed and permit an endothelial/stem cell fate.

regulation of primitive hematopoiesis have remained elusive. Here, we use multiple *lsd1*-mutant alleles that have similar levels of impaired catalytic activity but differential effects on rescuing *lsd1* mutant primitive hematopoiesis, with SNAG peptides to interfere with the LSD1 substrate-binding pocket, to show that (1) Lsd1 represses hematopoietic gene expression in a catalysis-independent manner, (2) the interaction between Lsd1 and Gfi1 creates a negative feedback loop that represses *gfi1* mRNA expression, and (3) the Lsd1 SNAG-binding and tower domains are critical for Lsd1-mediated transcriptional regulation during primitive hematopoiesis *in vivo*.

In this study, we show that loss of *lsd1* results in an upregulation of *gfi1ab* and a downregulation of *gata1*, similar to what we and others have observed with loss of *gfi1aa*.[42,52,53] These data suggest a model whereby Gfi1aa normally recruits Lsd1 to repress the expression of stem cell genes, such as *scl1*, *lmo2*, *tbx16* and *etv2,* in a common hemato-vascular mesoderm (HVM) cell, thereby providing a permissive landscape for driving cells toward primitive hematopoietic cell fates. Loss of, or interference with, either Lsd1 or Gfi1aa would then lead to elevated levels of stem cell genes in HVM cells, promoting a shift toward endothelial and/or HVM cell fates at the expense of primitive erythrocyte and myeloid cells. In this model, the reversible nature of SNAG-binding to LSD1 would allow for the repression of HVM stem cell genes to occur transiently, thereby ensuring such programs can be reactivated later in development.

An LSD1-SNAG-dependent negative feedback loop would represent an ideal mechanism for controlling oscillating gene expression programs in HVM cells. Indeed, it is known that SNAG family proteins negatively regulate their own gene expression, as well as expression of other members of their gene family, by unknown mechanisms.[33–39] In *lsd1*-mutant zebrafish, we found that Lsd1 negatively regulates GFI-family genes in the ICM, where primitive hematopoiesis takes place in the developing embryo. We also observed the upregulation of SNAIL-family genes in neural-crest-related tissues in *lsd1* zebrafish mutants, suggesting that LSD1 may also regulate SNAIL-mediated processes, such as neural crest development. This latter possibility was suggested in a recent study that showed upregulation of SNAI2 following LSD1 inhibition in epidermal progenitor cells.[54] LSD1 is also recruited by SNAIL1 and SNAIL2 to prompt the epithelial-to-mesenchymal transition (EMT), a process critical for both development and cancer progression.[49,55] Thus, LSD1 is likely to be intricately linked with diverse biological programs through its interactions with SNAG-family proteins, particularly during embryogenesis. It is likely that the design of *LSD1* mutant alleles that can effectively uncouple LSD1 demethylase activity from its substrate binding capacity will be necessary for understanding the role of LSD1 in controlling these feedback loops.

A model is emerging in which LSD1, GFI-family proteins and the BHC/CoREST complex function together to regulate transcriptional programs that drive hematopoiesis. We and others found that the BHC/CoREST complex is critical for GFI-family-mediated regulation of the hematopoietic lineage,[5,40] and the GFI-LSD1 interaction is required for AML cell survival.[6–9] In this study, we found that the LSD1 tower domain, which is important for binding to RCOR1 (a member of the BHC/CoREST and CtBP complexes), MTA1 and MTA2 (members of the NuRD complex), and SIN3A,[24,50,51] is critical for maintaining early hematopoietic programs. Although the BHC/CoREST complex is widely associated with the GFI family and hematopoietic lineage regulation,[5–8,18,40,56–60] links to the NuRD, CtBP, and Sin3A complexes have also been reported.[30,61–63] Future studies involving the use of LSD1-protein-partner mutants will clarify the complexes that are necessary for LSD1-mediated transcriptional programs that drive primitive hematopoiesis.

LSD1 has become a therapeutic target-of-interest because of its elevated expression in malignancies such as neuroblastoma, small-cell lung cancer, and leukemia.[64–66] Like-wise, SNAG-domain transcription factors, many whose functions in transcriptional control depend on LSD1, are emerging as critical determinants of malignant behavior. For example, GFI1 has pro-survival functions in both myeloid and lymphoid leukemias, in medulloblastoma and in the pre-malignant condition, severe congenital neutropenia.[67–70] Similarly, SNAIL family members figure prominently in the development and progression of breast cancer.[71,72] Inhibitors of LSD1 could therefore have broad reaching implications for cancer treatment. The first available inhibitors of LSD1 included tranylcypromine derivatives that irreversibly inactivate LSD1 through covalent modification of FAD.[73] However, disrupting interactions between LSD1 and its protein partners may be a more effective therapeutic strategy than inhibiting its catalytic activity. Indeed, uncoupling LSD1 from GFI1 or GFI1B alters cellular differentiation in cancer.[6,8,9,74,75] A better understanding of the catalysis-dependent and-independent functions of LSD1, the specific multiprotein complexes with which LSD1 interacts, the post-translational modifications of histones and other transcription factors governed by LSD1, the changes brought on by LSD1 inhibition, and the loci that LSD1 regulates will better inform

the design of effective therapeutic strategies targeting LSD1 and its SNAG domain transcription factor partners for cancer treatment.

Limitations of the study

LSD1/KDM1A is a multifaceted protein because of its ability to demethylate substrates (histones and transcription factors) and provide a scaffold to recruit various chromatin-modifying complexes. Unraveling the different functions of LSD1 will require methods that uncouple its enzymatic and structural functions for testing in both biochemical and *in vivo* assays. Previous studies have relied heavily on the use of one point mutation that abolishes LSD1's demethylase activity on mono- or di-methylated histone peptide substrates *in vitro*, called the K661A mutation. However, recent studies showed that the K661A mutation still retains 20% activity when reconstituted nucleosomes are used as substrate, limiting our ability to interpret LSD1's potential non-catalytic functions in prior cell- or animal-based experiments. Indeed, to our knowledge, there are no described LSD1 point mutations that completely uncouple its catalytic activity from its substrate binding capacity. The A539E point mutation used in this study was recently shown to have less than 5% catalytic activity on nucleosomes; however, this is likely because of its inability to effectively bind substrates because the hydrophobic pocket is disrupted by a charged residue. Therefore, based on LSD1 activity toward nucleosome substrates alone, our data could support the conclusion that LSD1 catalytic activity is required for controlling gene expression *in vivo*, as the K661A allele (20% activity) rescued Lsd1-mediated gene regulation but the A539E allele (5% activity) did not. For this reason, we also analyzed the ability of the D555K point mutation to rescue *lsd1* mutants, as D555K is located in the hydrophobic pocket and was reported to exhibit higher catalytic activity (>20%) than K661A on histone peptides,[23–25] although its activity on reconstituted nucleosomes is not known. The inability of D555K to restore *lsd1* mutant phenotypes bolsters the conclusion that the substrate-binding property of LSD1 is more critical than its catalytic activity during primitive hematopoietic development. This conclusion was further strengthened by the use of exogenous SNAG peptides to block wild-type LSD1 function *in vivo*. However, at this time our data cannot rule out an alternative model in which both substrate binding and a threshold level of LSD1 catalytic activity (between 5 and 20%) is required for control of gene expression programs *in vivo*. To address this possibility, biochemical assays using nucleosomes as substrates will be required in combination with new LSD1 mutants that can clearly uncouple catalytic activity from substrate binding. Nonetheless, our studies show that LSD1 substrate binding, particularly to SNAG-domain-containing transcription factors, is a prerequisite for mediating LSD1's function *in vivo*, regardless of whether LSD1 catalytic activity is required.

STAR★METHODS

Detailed methods are provided in the online version of this paper and include the following:

- KEY RESOURCES TABLE
- RESOURCE AVAILABILITY
  - Lead contact
  - Materials availability
  - Data and code availability
- EXPERIMENTAL MODEL AND SUBJECT DETAILS
  - Ethics statement
  - Zebrafish husbandry
- METHOD DETAILS
  - Molecular biology and cloning
  - Genomic DNA extraction and high-melt-resolution analysis (HRMA)
  - Microinjection
  - Whole-mount *in situ* hybridization (WISH)
  - RNA sequencing
  - Whole-mount antibody staining
  - Protein lysates and western blotting
  - CRISPR/Cas9
  - Image acquisition and processing
  - Statistical analysis

SUPPLEMENTAL INFORMATION

Supplemental information can be found online at https://doi.org/10.1016/j.isci.2022.105737.

ACKNOWLEDGMENTS

We thank Katherine E. Varley for critical reading of this manuscript, the H. Joseph Yost laboratory for reagents, David J. Grunwald for reagents and technical support, David McClellan for sgRNA design assistance, and Chris Stubben for help with RNA sequencing analysis. Research reported in this publication utilized the High-Throughput Genomics and Bioinformatic Analysis Shared Resource at the University of Utah Huntsman Cancer Institute, which is supported by the National Cancer Institute (P30CA042014) as well as the University of Utah Mutation Generation and Detection Core. We thank current and former members of the RAS and MEE laboratories for thoughtful discussions, and the Huntsman Cancer Institute/University of Utah Zebrafish Facility for providing animal husbandry. This work was supported by funding from the National Institutes of Health (R01NS106527, P30CA042014) (RAS), (R01CA201235) (MEE), T32 DK007115 (MJC) as well as the Huntsman Cancer Foundation and the Hyundai Hope on Wheels Foundation.

AUTHOR CONTRIBUTIONS

This study was conceived and designed by M.J.C., R.A.S., and M.E.E. M.J.C. and A.M.C. performed the experiments. M.J.C., A.M.C., A.V.T., and R.A.S. analyzed the data. The manuscript was prepared by M.J.C., C.A.J., and R.A.S. with input from all authors.

DECLARATION OF INTERESTS

The authors declare no conflicts of interest.

Received: April 4, 2022
Revised: September 15, 2022
Accepted: December 1, 2022
Published: January 20, 2023

REFERENCES

1. Shi, Y., Lan, F., Matson, C., Mulligan, P., Whetstine, J.R., Cole, P.A., Casero, R.A., and Shi, Y. (2004). Histone demethylation mediated by the nuclear amine oxidase homolog LSD1. Cell *119*, 941–953. https://doi.org/10.1016/j.cell.2004.12.012.

2. Metzger, E., Wissmann, M., Yin, N., Müller, J.M., Schneider, R., Peters, A.H.F.M., Günther, T., Buettner, R., and Schüle, R. (2005). LSD1 demethylates repressive histone marks to promote androgen-receptor-dependent transcription. Nature *437*, 436–439. https://doi.org/10.1038/nature04020.

3. Huang, J., Sengupta, R., Espejo, A.B., Lee, M.G., Dorsey, J.A., Richter, M., Opravil, S., Shiekhattar, R., Bedford, M.T., Jenuwein, T., and Berger, S.L. (2007). P53 is regulated by the lysine demethylase LSD1. Nature *449*, 105–108. https://doi.org/10.1038/nature06092.

4. Kontaki, H., and Talianidis, I. (2010). Lysine methylate regulates E2F1-induced cell death. Mol. Cell *39*, 152–160. https://doi.org/10.1016/j.molcel.2010.06.006.

5. McClellan, D., Casey, M.J., Bareyan, D., Lucente, H., Ours, C., Velinder, M., Singer, J., Lone, M.D., Sun, W., Coria, Y., et al. (2019). Growth factor independence 1B-mediated transcriptional repression and lineage allocation require lysine-specific demethylase 1-dependent recruitment of the BHC complex. Mol. Cell Biol. *39*, 000200–e119. https://doi.org/10.1128/MCB.00020-19.

6. Maiques-Diaz, A., Spencer, G.J., Lynch, J.T., Ciceri, F., Williams, E.L., Amaral, F.M.R., Wiseman, D.H., Harris, W.J., Li, Y., Sahoo, S., et al. (2018). Enhancer activation by pharmacologic displacement of LSD1 from GFI1 induces differentiation in acute myeloid leukemia. Cell Rep. *22*, 3641–3659. https://doi.org/10.1016/j.celrep.2018.03.012.

7. Vinyard, M.E., Su, C., Siegenfeld, A.P., Waterbury, A.L., Freedy, A.M., Gosavi, P.M., Park, Y., Kwan, E.E., Senzer, B.D., Doench, J.G., et al. (2019). CRISPR-suppressor scanning reveals a nonenzymatic role of LSD1 in AML. Nat. Chem. Biol. *15*, 529–539. https://doi.org/10.1038/s41589-019-0263-0.

8. Yamamoto, R., Kawahara, M., Ito, S., Satoh, J., Tatsumi, G., Hishizawa, M., Suzuki, T., and Andoh, A. (2018). Selective dissociation between LSD1 and GFI1B by a LSD1 inhibitior NCD38 induces the activation of ERG super-enhancer in erythroleukemia cells. Oncotarget *9*, 21007–21021. https://doi.org/10.18632/oncotarget.24774.

9. Barth, J., Abou-El-Ardat, K., Dalic, D., Kurrle, N., Maier, A.M., Mohr, S., Schütte, J., Vassen, L., Greve, G., Schulz-Fincke, J., et al. (2019). LSD1 inhibition by tranylcypromine derivatives interferes with GFI1-mediated repression of PU.1 target genes and induces differentiation in AML. Leukemia *33*, 1411–1426. https://doi.org/10.1038/s41375-018-0375-7.

10. Carnesecchi, J., Cerutti, C., Vanacker, J.M., and Forcet, C. (2017). ERRα protein is stabilized by LSD1 in a demethylation-independent manner. PLoS One *12*, e0188871. https://doi.org/10.1371/journal.pone.0188871.

11. Sehrawat, A., Gao, L., Wang, Y., Bankhead, A., 3rd, McWeeney, S.K., King, C.J., Schwartzman, J., Urrutia, J., Bisson, W.H., Coleman, D.J., et al. (2018). LSD1 activates a lethal prostate cancer gene network independently of its demethylase function. Proc. Natl. Acad. Sci. USA *115*, 4179–4188. https://doi.org/10.1073/pnas.1719168115.

12. de Jong, J.L.O., and Zon, L.I. (2005). Use of the zebrafish system to study primitive and definitive hematopoiesis. Annu. Rev. Genet. *39*, 481–501. https://doi.org/10.1146/annurev.genet.39.073003.095931.

13. Stachura, D.L., and Traver, D. (2016). Cellular dissection of zebrafish hematopoiesis. Methods Cell Biol. *133*, 11–53. https://doi.org/10.1016/bs.mcb.2016.03.022.

14. Kwan, W., and North, T.E. (2017). Netting novel regulators of hematopoiesis and hematologic malignancies in zebrafish. Curr.Top. Dev. Biol. *124*, 125–160. https://doi.org/10.1016/bs.ctdb.2016.11.005.

15. Maiques-Diaz, A., and Somervaille, T.C. (2016). LSD1: biologic roles and therapeutic targeting. Epigenomics *8*, 1103–1116. https://doi.org/10.2217/epi-2016-0009.

16. Sprüssel, A., Schulte, J.H., Weber, S., Necke, M., Händschke, K., Thor, T., Pajtler, K.W., Schramm, A., König, K., Diehl, L., et al. (2012). Lysine-specific demethylase 1 restricts hematopoietic progenitor proliferation and is essential for terminal differentiation.

Leukemia *26*, 2039–2051. https://doi.org/10.1038/leu.2012.157.

17. Kerenyi, M.A., Shao, Z., Hsu, Y.J., Guo, G., Luc, S., O'Brien, K., Fujiwara, Y., Peng, C., Nguyen, M., and Orkin, S.H. (2013). Histone demethylase Lsd1 represses hematopoietic stem and progenitor cell signatures during blood cell maturation. Elife *2*, e00633. https://doi.org/10.7554/eLife.00633.

18. Thambyrajah, R., Mazan, M., Patel, R., Moignard, V., Stefanska, M., Marinopoulou, E., Li, Y., Lancrin, C., Clapes, T., Möröy, T., et al. (2016a). GFI1 proteins orchestrate the emergence of haematopoietic stem cells through recruitment of LSD1. Nat. Cell Biol. *18*, 21–32. https://doi.org/10.1038/ncb3276.

19. Takeuchi, M., Fuse, Y., Watanabe, M., Andrea, C.S., Takeuchi, M., Nakajima, H., Ohashi, K., Kaneko, H., Kobayashi-Osaki, M., Yamamoto, M., and Kobayashi, M. (2015). LSD1/KDM1A promotes hematopoietic commitment of hemangioblasts through downregulation of Etv2. Proc. Natl. Acad. Sci. USA *112*, 13922–13927. https://doi.org/10.1073/pnas.1517326112.

20. Tamaoki, J., Takeuchi, M., Abe, R., Kaneko, H., Wada, T., Hino, S., Nakao, M., Furukawa, Y., and Kobayashi, M. (2020). Splicing- and demethylase-independent functions of LSD1 in zebrafish primitive hematopoiesis. Sci. Rep. *10*, 8521. https://doi.org/10.1038/s41598-020-65428-9.

21. Wang, J., Scully, K., Zhu, X., Cai, L., Zhang, J., Prefontaine, G.G., Krones, A., Ohgi, K.A., Zhu, P., Garcia-Bassets, I., et al. (2007). Opposing LSD1 complexes function in developmental gene activation and repression programmes. Nature *446*, 882–887. https://doi.org/10.1038/nature05671.

22. Wang, J., Hevi, S., Kurash, J.K., Lei, H., Gay, F., Bajko, J., Su, H., Sun, W., Chang, H., Xu, G., et al. (2009). The lysine demethylase LSD1 (KDM1) is required for maintenance of global DNA methylation. Nat. Genet. *41*, 125–129. https://doi.org/10.1038/ng.268.

23. Kim, S.A., Zhu, J., Yennawar, N., Eek, P., and Tan, S. (2020). Crystal structure of the LSD1/CoREST histone demethylase bound to its nucleosome substrate. Mol. Cell *78*, 903–914.e4. https://doi.org/10.1016/j.molcel.2020.04.019.

24. Chen, Y., Yang, Y., Wang, F., Wan, K., Yamane, K., Zhang, Y., and Lei, M. (2006). Crystal structure of human histone lysine-specific demethylase 1 (LSD1). Proc. Natl. Acad. Sci. USA *103*, 13956–13961. https://doi.org/10.1073/pnas.0606381103.

25. Stavropoulos, P., Blobel, G., and Hoelz, A. (2006). Crystal structure and mechanism of human lysine-specific demethylase-1. Nat. Struct. Mol. Biol. *13*, 626–632. https://doi.org/10.1038/nsmb1113.

26. Lin, Y., Wu, Y., Li, J., Dong, C., Ye, X., Chi, Y.I., Evers, B.M., and Zhou, B.P. (2010a). The SNAG domain of Snail1 functions as a molecular hook for recruiting lysine-specific demethylase 1. EMBO J. *29*, 1803–1816. https://doi.org/10.1038/emboj.2010.63.

27. Baron, R., Binda, C., Tortorici, M., McCammon, J.A., and Mattevi, A. (2011). Molecular mimicry and ligand recognition in binding and catalysis by the histone demethylase LSD1-CoREST complex. Structure *19*, 212–220. https://doi.org/10.1016/j.str.2011.01.001.

28. Beauchemin, H., and Möröy, T. (2020). Multifaceted actions of GFI1 and GFI1B in hematopoietic stem cell self-renewal and lineage commitment. Front. Genet. *11*, 591099. https://doi.org/10.3389/fgene.2020.591099.

29. Nieto, M.A. (2002). The snail superfamily of zinc-finger transcription factors. Nat. Rev. Mol. Cell Biol. *3*, 155–166. https://doi.org/10.1038/nrm757.

30. Shooshtarizadeh, P., Helness, A., Vadnais, C., Brouwer, N., Beauchemin, H., Chen, R., Bagci, H., Staal, F.J.T., Coté, J.F., and Möröy, T. (2019). Gfi1b regulates the level of Wnt/β-catenin signaling in hematopoietic stem cells and megakaryocytes. Nat. Commun. *10*, 1270. https://doi.org/10.1038/s41467-019-09273-z.

31. Möröy, T., Vassen, L., Wilkes, B., and Khandanpour, C. (2015). From cytopenia to leukemia: the role of Gfi1 and Gfi1b in blood formation. Blood *126*, 2561–2569. https://doi.org/10.1182/blood-2015-06-655043.

32. van der Meer, L.T., Jansen, J.H., and van der Reijden, B.A. (2010). Gfi1 and Gfi1b: key regulators of hematopoiesis. Leukemia *24*, 1834–1843. https://doi.org/10.1038/leu.2010.195.

33. Doan, L.L., Porter, S.D., Duan, Z., Flubacher, M.M., Montoya, D., Tsichlis, P.N., Horwitz, M., Gilks, C.B., and Grimes, H.L. (2004). Targeted transcriptional repression of Gfi1 by GFI1 and GFI1B in lymphoid cells. Nucleic Acids Res. *32*, 2508–2519. https://doi.org/10.1093/nar/gkh570.

34. Yücel, R., Kosan, C., Heyd, F., and Möröy, T. (2004). Gfi1:Green fluorescent protein knock-in mutant reveals different expression and autoregulation of the growth factor independence 1 (Gfi1) gene during lymphocyte development. J. Biol. Chem. *279*, 40906–40917. https://doi.org/10.1074/jbc.M400808200.

35. Huang, D.Y., Kuo, Y.Y., and Chang, Z.F. (2005). GATA-1 mediates auto-regulation of Gfi-1B transcription in K562 cells. Nucleic Acids Res. *33*, 5331–5342. https://doi.org/10.1093/nar/gki838.

36. Vassen, L., Fiolka, K., Mahlmann, S., and Möröy, T. (2005). Direct transcriptional repression of genes encoding the zinc-finger proteins Gfi1b and Gfi1 by Gfi1b. Nucleic Acids Res. *33*, 987–998. https://doi.org/10.1093/nar/gki243.

37. Anguita, E., Villegas, A., Iborra, F., and Hernández, A. (2010). GFI1B controls its own expression binding to multiple sites. Haematologica *95*, 36–46. https://doi.org/10.3324/haematol.2009.012351.

38. Boettiger, A.N., and Levine, M. (2013). Rapid transcription kinetics foster coordinate snail expression in the Drosophila embryo. Cell Rep. *3*, 8–15. https://doi.org/10.1016/j.celrep.2012.12.015.

39. Sundararajan, V., Tan, M., Tan, T.Z., Ye, J., Thiery, J.P., and Huang, R.Y.J. (2019). SNAI1 recruits HDAC1 to suppress SNAI2 transcription during epithelial to mesenchymal transition. Sci. Rep. *9*, 8295. https://doi.org/10.1038/s41598-019-44826-8.

40. Saleque, S., Kim, J., Rooke, H.M., and Orkin, S.H. (2007). Epigenetic regulation of hematopoietic differentiation by Gfi-1 and Gfi-1b is mediated by the cofactors CoREST and LSD1. Mol. Cell *27*, 562–572. https://doi.org/10.1016/j.molcel.2007.06.039.

41. Busch-Nentwich, E., Kettleborough, R., Dooley, C.M., Scahill, C., Sealy, I., White, R., Herd, C., Mehroke, S., Wali, N., Carruthers, S., et al. (2013). Sanger Institute Zebrafish Mutation Project Mutant Data Submission (ZFIN Direct Data Submission).

42. Grimes, H.L., Chan, T.O., Zweidler-McKay, P.A., Tong, B., and Tsichlis, P.N. (1996). The Gfi-1 proto-oncoprotein contains a novel transcriptional repressor domain, SNAG, and inhibits G1 arrest induced by interleukin-2 withdrawal. Mol. Cell Biol. *16*, 6263–6272. https://doi.org/10.1128/mcb.16.11.6263.

43. Cooney, J.D., Hildick-Smith, G.J., Shafizadeh, E., McBride, P.F., Carroll, K.J., Anderson, H., Shaw, G.C., Tamplin, O.J., Branco, D.S., Dalton, A.J., et al. (2013). Teleost growth factor independence (gfi) genes differentially regulate successive waves of hematopoiesis. Dev. Biol. *373*, 431–441. https://doi.org/10.1016/j.ydbio.2012.08.015.

44. Dufourcq, P., Rastegar, S., Strähle, U., and Blader, P. (2004). Parapineal specific expression of gfi1 in the zebrafish epithalamus. Gene Expr. Patterns *4*, 53–57. https://doi.org/10.1016/s1567-133x(03)00148-0.

45. Wu, M., Chen, Q., Li, J., Xu, Y., Lian, J., Liu, Y., Meng, P., and Zhang, Y. (2021). Gfi1aa/Lsd1 facilitates hemangioblast differentiation into primitive erythrocytes by targeting etv2 and sox7 in zebrafish. Front. Cell Dev. Biol. *9*, 786426. https://doi.org/10.3389/fcell.2021.786426.

46. Fraaije, M.W., and Mattevi, A. (2000). Flavoenzymes: diverse catalysts with recurrent features. Trends Biochem. Sci. *25*, 126–132. https://doi.org/10.1016/s0968-0004(99)01533-9.

47. Forneris, F., Binda, C., Vanoni, M.A., Mattevi, A., and Battaglioli, E. (2005). Histone demethylation catalyzed by LSD1 is a flavin-dependent oxidative process. FEBS Lett. *579*, 2203–2207. https://doi.org/10.1016/j.febslet.2005.03.0.

48. Velinder, M., Singer, J., Bareyan, D., Meznarich, J., Tracy, C.M., Fulcher, J.M., McClellan, D., Lucente, H., Franklin, S., Sharma, S., and Engel, M.E. (2016). GFI1 functions in transcriptional control and cell fate determination require SNAG domain methylation to recruit LSD1. Biochem. J. *473*, 3355–3369. https://doi.org/10.1042/BCJ20160558.

49. Ferrari-Amorotti, G., Fragliasso, V., Esteki, R., Prudente, Z., Soliera, A.R., Cattelani, S., Manzotti, G., Grisendi, G., Dominici, M., Pieraccioli, M., et al. (2013). Inhibiting interactions of lysine demethylase LSD1 with Snail/Slug blocks cancer cell invasion. Cancer Res. *73*, 235–245. https://doi.org/10.1158/0008-5472.CAN-12-1739.

50. Wang, Y., Zhang, H., Chen, Y., Sun, Y., Yang, F., Yu, W., Liang, J., Sun, L., Yang, X., Shi, L., et al. (2009). LSD1 is a subunit of the NuRD complex and targets the metastasis programs in breast cancer. Cell *138*, 660–672. https://doi.org/10.1016/j.cell.2009.05.050.

51. Yang, Y., Huang, W., Qiu, R., Liu, R., Zeng, Y., Gao, J., Zheng, Y., Hou, Y., Wang, S., Yu, W., et al. (2018). LSD1 coordinates with the SIN3A/HDAC complex and maintains sensitivity to chemotherapy in breast cancer. J. Mol. Cell Biol. *10*, 285–301. https://doi.org/10.1093/jmcb/mjy021.

52. Moore, C., Richens, J.L., Hough, Y., Ucanok, D., Malla, S., Sang, F., Chen, Y., Elworthy, S., Wilkinson, R.N., and Gering, M. (2018). Gfi1aa and gfi1b set the pace for primitive erythroblast differentiation from hemangioblasts in the zebrafish embryo. Blood Adv. *2*, 2589–2606. https://doi.org/10.1182/bloodadvances.2018020156.

53. Thambyrajah, R., Ucanok, D., Jalali, M., Hough, Y., Wilkinson, R.N., McMahon, K., Moore, C., and Gering, M. (2016b). A gene trap transposon eliminates hematopoietic expression of zebrafish Gfi1aa, but does not interfere with hematopoiesis. Dev. Biol. *417*, 25–39. https://doi.org/10.1016/j.ydbio.2016.07.010.

54. Egolf, S., Aubert, Y., Doepner, M., Anderson, A., Maldonado-Lopez, A., Pacella, G., Lee, J., Ko, E.K., Zou, J., Lan, Y., et al. (2019). LSD1 inhibition promotes epithelial differentiation through derepression of fate-determining transcription factors. Cell Rep. *28*, 1981–1992.e7. https://doi.org/10.1016/j.celrep.2019.07.058.

55. Lin, T., Ponn, A., Hu, X., Law, B.K., and Lu, J. (2010b). Requirement of the histone demethylase LSD1 in Snail1-mediated transcriptional repression during epithelial-mesenchymal transition. Oncogene *29*, 4896–4904. https://doi.org/10.1038/onc.2010.234.

56. Laurent, B., Randrianarison-Huetz, V., Frisan, E., Andrieu-Soler, C., Soler, E., Fontenay, M., Dusanter-Fourt, I., and Duménil, D. (2012). A short GFI-1B isoform controls erythroid differentiation by recruiting the LSD1-CoREST complex through the dimethylationn of its SNAG domain. J. Cell Sci. *125*, 993–1002. https://doi.org/10.1242/jcs.095877.

57. Laurent, B., Randrianarison-Huetz, V., Kadri, Z., Roméo, P.H., Porteu, F., and Duménil, D. (2009). Gfi-1B promoter remains associated with active chromatin marks throughout erythroid differentiation of human primary progenitor cells. Stem Cell. *27*, 2153–2162. https://doi.org/10.1002/stem.151.

58. Tatsumi, G., Kawahara, M., Yamamoto, R., Hishizawa, M., Kito, K., Suzuki, T., Takaori-Kondo, A., and Andoh, A. (2020). LSD1-mediated repression of GFI1 super-enhancer plays an essential role in erythroleukemia. Leukemia *34*, 746–758. https://doi.org/10.1038/s41375-019-0614-6.

59. Chowdhury, A.H., Ramroop, J.R., Upadhyay, G., Sengupta, A., Andrzejczyk, A., and Saleque, S. (2013). Differential transcriptional regulation of meis1 by Gfi1b and its co-factors LSD1 and CoREST. PLoS One *8*, e53666. https://doi.org/10.1371/journal.pone.0053666.

60. Andrade, D., Velinder, M., Singer, J., Maese, L., Bareyan, D., Nguyen, H., Chandrasekharan, M.B., Lucente, H., McClellan, D., Jones, D., et al. (2016). SUMOylation regulates growth factor independence 1 in transcriptional control and hematopoiesis. Mol. Cell Biol. *36*, 1438–1450. https://doi.org/10.1128/MCB.01001-15.

61. Ross, J., Mavoungou, L., Bresnick, E.H., and Milot, E. (2012). GATA-1 utilizes Ikaros and polycomb repressive complex 2 to suppress Hes1 and to promote erythropoiesis. Mol. Cell Biol. *32*, 3624–3638. https://doi.org/10.1128/MCB.00163-12.

62. Hamlett, I., Draper, J., Strouboulis, J., Iborra, F., Porcher, C., and Vyas, P. (2008). Characterization of megakaryocyte GATA1-interacting proteins: the corepressor ETO2 and GATA1 interact to regulate terminal megakaryocyte maturation. Blood *112*, 2738–2749. https://doi.org/10.1182/blood-2008-03-146605.

63. Jiang, X., Hu, C., Arnovitz, S., Bugno, J., Yu, M., Zuo, Z., Chen, P., Huang, H., Ulrich, B., Gurbuxani, S., et al. (2016). miR-22 has a potent anti-tumour role with therapeutic potential inn acute myeloid leukaemia. Nat. Commun. *7*, 11452. https://doi.org/10.1038/ncomms11452.

64. Schulte, J.H., Lim, S., Schramm, A., Friedrichs, N., Koster, J., Versteeg, R., Ora, I., Pajtler, K., Klein-Hitpass, L., Kuhfittig-Kulle, S., et al. (2009). Lysine-specific demethylase 1 is strongly expressed in poorly differentiated neuroblastoma: implications for therapy. Cancer Res. *69*, 2065–2071. https://doi.org/10.1158/0008-5472.CAN-08-1735.

65. Lv, T., Yuan, D., Miao, X., Lv, Y., Zhan, P., Shen, X., and Song, Y. (2012). Over-expression of LSD1 promotes proliferation, migration and invasion in non-small cell lung cancer. PLoS One *7*, e35065. https://doi.org/10.1371/journal.pone.0035065.

66. Harris, W.J., Huang, X., Lynch, J.T., Spencer, G.J., Hitchin, J.R., Li, Y., Ciceri, F., Blaser, J.G., Greystoke, B.F., Jordan, A.M., et al. (2012). The histone demethylase KDM1A sustains the oncogenic potential of MLL-AF9 leukemia stem cells. Cancer Cell *21*, 473–487. https://doi.org/10.1016/j.ccr.2012.03.014.

67. Khandanpour, C., Thiede, C., Valk, P.J.M., Sharif-Askari, E., Nückel, H., Lohmann, D., Horsthemke, B., Siffert, W., Neubauer, A., Grzeschik, K.H., et al. (2010). A variant allele of growth factor independence 1 (GFI1) is associated with acute myeloid leukemia. Blood *115*, 2462–2472. https://doi.org/10.1182/blood-2009-08-239822.

68. Khandanpour, C., Phelan, J.D., Vassen, L., Schütte, J., Chen, R., Horman, S.R., Gaudreau, M.C., Krongold, J., Zhu, J., Paul, W.E., et al. (2013). Growth factor independence 1 antagonizes a p53-induced DNA damage response pathway in lymphoblastic leukemia. Cancer Cell *23*, 200–214. https://doi.org/10.1016/j.ccr.2013.01.011.

69. Northcott, P.A., Lee, C., Zichner, T., Stütz, A.M., Erkek, S., Kawauchi, D., Shih, D.J.H., Hovestadt, V., Zapatka, M., Sturm, D., et al. (2014). Enhancer hijacking activates GFI1 family oncogenes in medulloblastoma. Nature *511*, 428–434. https://doi.org/10.1038/nature13379.

70. Person, R.E., Li, F.Q., Duan, Z., Benson, K.F., Wechsler, J., Papadaki, H.A., Eliopoulos, G., Kaufman, C., Bertolone, S.J., Nakamoto, B., et al. (2003). Mutations in proto-oncogene GFI1 cause human neutropenia and target ELA2. Nat. Genet. *34*, 308–312. https://doi.org/10.1038/ng1170.

71. Fujita, N., Jaye, D.L., Kajita, M., Geigerman, C., Moreno, C.S., and Wade, P.A. (2003). MTA3, a Mi-2/NuRD complex subunit, regulates an invasive growth pathway in breast cancer. Cell *113*, 207–219. https://doi.org/10.1016/s0092-8674(03)00234-4.

72. Côme, C., Magnino, F., Bibeau, F., De Santa Barbara, P., Becker, K.F., Theillet, C., and Savagner, P. (2006). Snail and slug play distinct roles during breast carcinoma progression. Clin. Cancer Res. *12*, 5395–5402. https://doi.org/10.1158/1078-0432.CCR-06-0478.

73. Mould, D.P., McGonagle, A.E., Wiseman, D.H., Williams, E.L., and Jordan, A.M. (2015). Reversible inhibitors of LSD1 as therapeutic agents in acute myeloid leukemia: clinical significance and progress to date. Med. Res. Rev. *35*, 586–618. https://doi.org/10.1002/med.21334.

74. Fiskus, W., Sharma, S., Shah, B., Portier, B.P., Devaraj, S.G.T., Liu, K., Iyer, S.P., Bearss, D., and Bhalla, K.N. (2014). Highly effective combination of LSD1 (KDM1A) antagonist and pan-histone deacetylase inhibitor against human AML cells. Leukemia *28*, 2155–2164. https://doi.org/10.1038/leu.2014.119.

75. Sun, W., Guo, J., McClellan, D., Poeschla, A., Bareyan, D., Casey, M.J., Cairns, B.R., Tantin, D., and Engel, M.E. (2022). GFI1 cooperates with IKZF1/IKAROS to activate gene expression in T-cell acute lymphoblastic leukemia. Mol. Cancer Res. *20*, 501–514. https://doi.org/10.1158/1541-7786.

76. Detrich, H.W., Kieran, M.W., Chan, F.Y., Barone, L.M., Yee, K., Rundstadler, J.A., Pratt, S., Ransom, D., and Zon, L.I. (1995). Intraembryonic hematopoietic cell migration during vertebrate development. Proc. Natl. Acad. Sci. USA *92*, 10713–10717. https://doi.org/10.1073/pnas.92.23.10713.

77. Sumanas, S., Jorniak, T., and Lin, S. (2005). Identification of novel vascular endothelial-specific genes by the microarray analysis of the zebrafish cloche mutants. Blood *106*, 534–541. https://doi.org/10.1182/blood-200401204653.

78. Thisse, C., Thisse, B., Schilling, T.F., and Postlethwait, J.H. (1993). Structure of the zebrafish snail1 gene and its expression in wild-type, spadetail and no tail mutant embryos. Development *119*, 1203–1215. https://doi:10.1242/dev.119.4.1203.

79. Thisse, C., Thisse, B., and Postlethwait, J.H. (1995). Expression of snail2, a second member of the zebrafish snail family, in cephalic mesendoderm and presumptive neural crest of wild-type and spadetail mutant embryos. Dev. Biol. *172*, 86–99. https://doi.org/10.1006/dbio.1995.0007.

80. Thisse, B., Pflumio, S., Furthauer, M., Loppin, B., Heyer, V., Degrave, A., Woehl, R., Lux, A., Steffan, T., Charbonnier, X.Q., and Thisse, C. (2001). Expression of the Zebrafish Genome during Embryogenesis (ZFIN Direct Data Submission).

81. Westerfield, M. (1993). The Zebrafish Book (University of Oregon Press).

82. Draper, B.W., McCallum, C.M., and Moens, C.B. (2007). Nanos1 is required to maintain oocyte production in adult zebrafish. Dev. Biol. *305*, 589–598. https://doi.org/10.1016/j.ydbio.2007.03.007.

83. Dahlem, T.J., Hoshijima, K., Jurynec, M.J., Gunther, D., Starker, C.G., Locke, A.S., Weis, A.M., Voytas, D.F., and Grunwald, D.J. (2012). Simple methods for generating and detecting locus-specific mutations induced with TALENs in the zebrafish genome. PLoS Genet. *8*, e1002861. https://doi.org/10.1371/journal.pgen.1002861.

84. Xing, L., Quist, T.S., Stevenson, T.J., Dahlem, T.J., and Bonkowsky, J.L. (2014). Rapid and efficient zebrafish genotyping using PCR with high-resolution melt analysis. J. Vis. Exp. e51138. https://doi.org/10.3791/51138.

85. Boer, E.F., Howell, E.D., Schilling, T.F., Jette, C.A., and Stewart, R.A. (2015). Fascin1-dependent filopodia are required for directional migration of a subset of neural crest cells. PLoS Genet. *11*, e1004946. https://doi.org/10.1371/journal.pgen.1004946.

86. Love, M.I., Huber, W., and Anders, S. (2014). Moderated estimation of fold change and dispersion for RNA-seq data with DESeq2. Genome Biol. *15*, 550. https://doi.org/10.1186/s13059-014-0550-8.

87. Robinson, J.T., Thorvaldsdóttir, H., Winckler, W., Guttman, M., Lander, E.S., Getz, G., and Mesirov, J.P. (2011). Integrative genomics viewer. Nat. Biotechnol. *29*, 24–26. https://doi.org/10.1038/nbt.1754.

88. Sorrells, S., Toruno, C., Stewart, R.A., and Jette, C. (2013). Analysis of apoptosis in zebrafish embryos by whole-mount immunofluorescence to detect activated Caspase 3. J. Vis. Exp. e51060. https://doi.org/10.3791/51060.

89. Amsterdam, A., Nissen, R.M., Sun, Z., Swindell, E.C., Farrington, S., and Hopkins, N. (2004). Identification of 315 genes essential for early zebrafish development. Proc. Natl. Acad. Sci. USA *101*, 12792–12797. https://doi.org/10.1073/pnas.0403929101.

STAR★METHODS

KEY RESOURCES TABLE

REAGENT or RESOURCE	SOURCE	IDENTIFIER
Antibodies		
Anti-Caspase 3	BD Bioscience	RRID: AB_397274; Cat#559565
Donkey Anti-Rabbit Alexa Fluor 568	Life Technologies	RRID: AB_2534017; Cat#A10042
Anti-Digoxigenin	Sigma Aldrich	RRID: AB_2734716; Cat#11093274910
Anti-Flag M2	Sigma Aldrich	RRID: AB_259529; Cat#F3165
HRP-Donkey Anti-Mouse IgG	Jackson Immunoresearch	RRID: AB_2340770; Cat#715-035-150
Anti-Phospho-Histone H3	Cell Signaling Technology	RRID: AB_331535; Cat#9701
Chemicals, peptides, and recombinant proteins		
SNAG peptide	GenScript	N/A
Proteinase K	Sigma Aldrich	Cat#RPROTK-RO
Ambion SP6 RNA Polymerase	Invitrogen	Cat#AM2071
Ambion T7 RNA Polymerase	Invitrogen	Cat#AM2082
Ribonucleic Acid Type VI	Sigma Aldrich	Cat#R6625
Heparin	Sigma Aldrich	Cat#H3393
Maleic Acid	Sigma Aldrich	Cat#M0375
Blocking Reagent	Roche	Cat#11096176001
Fetal Bovine Serum, Heat Inactivated	Gibco	Cat#10438026
RNAlater	Qiagen	Cat#76104
Phusion High-Fidelity DNA Polymerase	NEB	Cat#M0530S
Protease Inhibitor Cocktail	Sigma Aldrich	Cat#P8340
gfi1b sgRNA	This paper	N/A
Critical commercial assays		
OneStep RT-PCR	Qiagen	Cat#210210
QuikChange II Site-Directed Mutagenesis Kit	Agilent	Cat#200523
QIAquick Gel Extraction Kit	Qiagen	Cat#28704
pGEM-T-Easy Vector Systems	Promega	Cat#A1360
LightScanner Master Mix	BioFire Defense	Cat#HRLS-ASY-0003
mMessage mMachine SP6 Transcription Kit	Invitrogen	Cat#AM1340
NucAway Spin Columns	Thermo Fisher	Cat#AM10070
DIG RNA Labeling Mix	Sigma Aldrich	Cat#11277073910
BCIP/NBT Substrate Kit	Vector Laboratories	Cat#SK5400
PureLink RNA MicroKit	Invitrogen	Cat#12183016
SuperSignal West Femto Maximum Sensitivity Substrate	Thermo Fisher	Cat#34095
Cas9	IDT	Cat#1081058
HiScribe T7 Quick High Yield RNA Synthesis RNA Kit	NEB	Cat#E2050S
RNeasy Plus Mini Kit	Qiagen	Cat#74134
Protease inhibitor cocktail	Sigma Aldrich	Cat#P8340
PVDF membrane	Millipore	Cat#IPVH00010

(*Continued on next page*)

Continued

REAGENT or RESOURCE	SOURCE	IDENTIFIER
SuperSignal West Femto Maximum Sensitivity Substrate	Thermo Fisher	Cat#34095
Autoradiography film	Genesee Scientific	Cat#30-507
Deposited data		
Raw data	This paper	GEO: GSE198476
Experimental models: Organisms/strains		
Zebrafish: *kdm1a 23095*		ZFIN: ZDB-ALT-131217-16908
Zebrafish: *kdm1a 36433*		ZFIN: ZDB-ALT-161003-15414
Zebrafish: *gfi1aa 16850*		ZFIN: ZDB-ALT-131217-13025
Zebrafish: *gfi1ab 40706*		ZFIN: ZDB-ALT-160601-6870
Zebrafish: *plrg1 hi3174aTg*		ZFIN: ZDB-ALT-040826-6
Zebrafish: *gfi1b Δ17*	This paper	N/A
Oligonucleotides		
Primers for genotyping, see Table S2	This paper	N/A
Primers for cDNA amplification, see Table S2	This paper	N/A
Primers for site directed mutagenesis, see Table S2	This paper	N/A
Recombinant DNA		
pUC57-zlsd1-3XFLAG	This paper	N/A
pUC57-zlsd1-K661A	This paper	N/A
pUC57-zlsd1-ΔQ632-3XFLAG	This paper	N/A
pUC57-zlsd1-D555K-3XFLAG	This paper	N/A
pUC57-zlsd1-A539E-3XFLAG	This paper	N/A
pUC57-zlsd1-ΔTower-3XFLAG	This paper	N/A
pUC57-zlsd1-ΔAOLC	This paper	N/A
pUC57-hLsd1-3XFLAG	This paper	N/A
pUC57-hLsd1-ΔAOLC	This paper	N/A
pGEM-T-Easy-gfi1b	This paper	N/A
pGEM-T-Easy-gfi1aa	This paper	N/A
pGEM-T-Easy-gfi1ab	This paper	N/A
pGEM-T-Easy-fli1a	This paper	N/A
pBluescript-gata1	Detrich et al.[76]	N/A
pUC57-etv2	Sumanas et al.[77]	N/A
pBK-snail1a	Thisse et al.[78]	N/A
pBK-snail1b	Thisse et al.[79]	N/A
pBS-IISK-snai2	Thisse et al.[80]	ZFIN: ZDB-EST-030328-40
Software and algorithms		
ImageJ		
LightScanner Call-IT	Idaho Technology Inc.	
Adobe Illustrator	Adobe	
Adobe Photoshop	Adobe	
Integrated Genomics Viewer	Broad Institute	
RStudio	RStudio	
Pymol	Schrodinger Inc.	
GraphPad Prism	Dotmatics	

RESOURCE AVAILABILITY

Lead contact

Further information and requests for resources and reagents should be directed to Rodney Stewart (rodney.stewart@utah.edu).

Materials availability

Plasmids generated in this study are available upon request from the lead contact.

Data and code availability

- Raw RNA sequencing data is publicly available and has been deposited at GEO under the accession number GEO: GSE198476. Analyzed RNA sequencing data is available via Table S4.
- This paper does not report any original code.
- Any additional information required to reanalyze the data reported in this paper is available from the lead contact upon request.

EXPERIMENTAL MODEL AND SUBJECT DETAILS

Ethics statement

All experiments involving zebrafish conformed to the regulatory standards and guidelines of the University of Utah Institutional Animal Care and Use Committee.

Zebrafish husbandry

Zebrafish were bred and maintained as described.[81] The *kdm1a(23095)*, *kdm1a(36433)*, *gfi1aa(16850)*, *gfi1ab(40706)*, and *plrg1(hi3174aTg)* lines were obtained from the Zebrafish International Resource Center (http://www.zebrafish.org/home/guide.php). The *gfi1b(Δ17)* line was generated as described below.

METHOD DETAILS

Molecular biology and cloning

The entire cDNA of *zlsd1* (GRCz11 transcript 201) and *hLSD1* (GRCh38 transcript 201) was synthesized by Genewiz into the pUC57 backbone with flanking SP6 and T7 promoter sequences. pUC57-*etv2* was synthesized from Genewiz as described by Sumanas et al.[77] Site-directed mutagenesis (Agilent 200523) was performed on pUC57-*zlsd1* to generate the K661A, ΔQ632, D555K, and A539E mutations. The reaction was carried out for 5 min at 95°C, 16 cycles of 30 s at 95°C, 30 s at 55°C, 12 min at 68°C, ending with 15 min at 68°C and cooling to 4°C. An annealing temperature of 62°C was used to generate the A539E mutation. Mutagenesis was confirmed by Sanger sequencing. pUC57-*zlsd1* was used as a template to generate *zlsd1-ΔTower* using Phusion DNA Polymerase (NEB M0530S). The reaction was carried out for 30 s at 98°C, 35 cycles of 10 s at 98°C, 30 s at 68.6°C, 45 s at 72°C, ending with 10 min at 72°C and cooling to 4°C. Deletion from Gln399 to Ser502 was confirmed by BsaI digest and Sanger sequencing.

The zebrafish *gfi1aa*, *gfi1ab*, *gfi1b*, and *fli1a* cDNAs were amplified from 24-hpf zebrafish RNA using the One-Step RT-PCR kit (Qiagen 210,210). The reaction was carried out for 30 min at 50°C, 15 min at 95°C, 35 cycles of 30 s at 94°C, 30 s at 55°C (*gfi1aa*, *gfi1ab*, *gfi1b*) or 60°C (*fli1a*), 80 s at 72°C, ending with 10 min at 72°C and cooling to 4°C. The amplicon was purified via gel extraction (Qiagen 28,704) and ligated to pGEM via the pGEM-T-Easy Vector System (Fisher Scientific PRA1360). To determine the orientation of each cDNA, pGEM-*gfi1aa* and pGEM-*gfi1ab* were digested with SacI, pGEM-*gfi1b* was digested with NdeI, and pGEM-*fli1a* was digested with AccI. Sanger sequencing was performed to validate results.

Genomic DNA extraction and high-melt-resolution analysis (HRMA)

Genomic DNA was extracted from adult zebrafish by fin clipping. Fins were lysed in alkaline lysis solution (25 mM NaOH, 0.2 mM EDTA) at 95°C for 2 h and the solution was neutralized with 40 mM Tris pH 5.0. Isolation of genomic DNA from embryo heads or whole embryos following WISH was modified from Draper et al.[82] Embryos were placed in HRMA lysis buffer (20 mM Tris pH 8.0, 50 mM KCl, 0.3% Tween 20, 0.3% NP-40, 0.5 mg/mL proteinase K (Sigma Aldrich RPROTK-RO)), incubated at 95°C for 20 min, 55°C for 75 min, and ending with 20 min at 95°C.

Genotyping was performed by HRMA to amplify a 96-bp and 86-bp product for *kdm1a(23095)* and *kdm1a(36433)*, respectively. Similarly, HRMA was used to amplify a 91-bp product for *gfi1aa(16850)*, a 98-bp product for *gfi1ab(40706)*, and a 106-bp product for *gfi1b(Δ17)*. Briefly, 20 μL of mineral oil was added to each well of a 96-well plate (BioRad HSP9665). Each reaction contained 2 μL of LightScanner master mix (Idaho Technologies HRLS-ASY-0003), 0.5 μM of each primer, and 1 μL of genomic DNA. The plate was covered with an optically transparent seal, centrifuged at 1800 rcf for 2 min, and cycled with the following conditions: denaturation at 96°C for 5 min; 55 cycles of 30 s at 96°C, 30 s at 68°C, 30 s at 72°C, ending with 3 min at 95°C and cooled to 4°C. Genotyping data were collected on a LightScanner (Idaho Technology) and analyzed with the LightScanner Call-IT Software as previously described.[83,84] Homozygous *kdm1a* mutants were distinguished from wild-type animals, as described by Boer et al.[85] All samples that grouped with known wild-type samples were mixed with 1–4 μL of wild-type reaction, heated to 95°C for 5 min, and reanalyzed on the LightScanner. HRMA genotyping results were validated by standard polymerase chain reaction (PCR) of genomic DNA and Sanger sequencing.

Microinjection

To generate capped sense mRNA, the *zlsd1-ΔAOLC* mRNA and the *hLSD1-ΔAOLC* plasmids were digested with EcoRV. The pUC57-*zlsd1* and pUC57-*hLSD1* plasmids were digested with StuI. All other constructs were linearized with NotI. Linearized plasmids (400 ng) were *in vitro* transcribed using the SP6 mMESSAGE mMACHINE kit (Life Technologies AM1340). mRNA was purified using NucAway spin columns (Life Technologies AM10070) and microinjected into the single cell of zebrafish embryos at a dosage of 50–65 ng.

SNAG domain peptides were synthesized by GenScript to >85% purity. Peptides were reconstituted according to manufacturer's instructions in water at a stock concentration of 1 mg/mL. Equal concentrations of peptide and *zlsd1-3XFLAG* mRNA were microinjected into the single cell of zebrafish embryos at a dosage of 50–65 ng.

Whole-mount *in situ* hybridization (WISH)

To generate antisense RNA probes, pGEM-*fli1a*, pGEM-*gfi1b*, pGEM-*gfi1aa*,pGEM-*gfi1ab* were digested with SacII. pBluescript-*gata1* was digested with XbaI,[76] pUC57-*etv2* with KpnI, pBK-*snail1a* with BamHI,[78]*snail1b* with XbaI,[79] and pUC57-*snai2* with NotI.[80] A total of 2 ug of digested plasmid was *in-vitro* transcribed with either SP6 (Invitrogen AM2071) (*fli1a, gfi1b, gfi1aa, gfi1ab, etv2*) or T7 (Invitrogen AM2082) (*gata1, snail1a, snail1b, snai2*) polymerase and labeled with digoxigenin (Sigma Aldrich 11277073910). Probes were purified on NucAway spin columns (Life Technologies AM10070).

WISH was performed in either biological duplicates or triplicates, as previously described.[78] Briefly, embryos were grown to the desired stage, dechorionated, and fixed overnight in 4% paraformaldehyde at 4°C. The following day embryos were rinsed three times in PBST (1X PBS with 0.1% Tween 20) and dehydrated overnight at −20°C in methanol. To rehydrate, embryos were washed three times in PBST and placed in prewarmed HYB(−) solution (50% formamide, 5X SSC, 0.1% Tween 20) for 15 min at 68-70°C while gently rocking. The HYB(−) solution was replaced with HYB(+) solution (HYB(−), 5 mg/mL Torula RNA Type VI (Sigma Aldrich R6625), 50 ug/ml heparin (Sigma Aldrich H3393)) and rocked for 1 h at 68-70°C. The RNA probe was added and hybridization was performed overnight at 68-70°C. Embryos were washed at 68-70°C in 2X SSCT (2X SSC, 0.1% Tween 20) with 50% formamide two times for 30 min each, one time for 15 min in 2X SSCT, and two times for 30 min each in 0.2X SSCT. Embryos were transferred to room temperature and washed three times for 5 min each in 1X MABT pH 7.5 (100 mM maleic acid (Sigma Aldrich M0375), 150 mM NaCl, 100 mM Tris pH 9.5, 0.1% Tween 20) and subsequently placed in blocking solution (MABT, 2% BMB blocking reagent (Sigma Aldrich 11096176001), 10% heat-inactivated fetal bovine serum (Fisher Scientific 10438026) for 1 h. Anti-digoxygenin FAB fragment antibody (Sigma Aldrich 11093274910) was added at a 1:5000 final dilution and rocked overnight at 4°C. The next day embryos were washed at room temperature in blocking solution for 30 min, 1X MABT for 1 h, 1X MABT for 30 min, and 0.1M Tris pH 9.5 three times for 5 min each. BCIP/NBT substrate (Vector Laboratories SK-5400) was added, and embryos were covered with aluminum foil and rocked at room temperature until stained. Following staining, embryos were rinsed in PBST two times for 5 min each to stop the reaction, gradually transferred to 80% glycerol and imaged. Embryos older than 30 hpf were initially treated with 10 μg/mL of proteinase K, rinsed three times with PBST and fixed again in 4% paraformaldehyde overnight at 4°C before beginning the dehydration step.

RNA sequencing

Embryos from a heterozygous incross of *kdm1a(23095)* or *kdm1a(36433)* were dissected at 24 hpf just posterior to the yolk sac. The head was used for genomic DNA extraction and HRMA while the tail was placed in RNA stabilization solution (QIAGEN 76104) until genotyping was completed. Three independent clutches were collected and five tails from homozygous *lsd1* mutants or wild-type siblings were combined per clutch. Tails were rinsed in 1X PBS and pelleted. Tissue homogenization and RNA isolation was performed using the PureLink RNA Micro kit (Invitrogen 12183016) according to manufacturer's instructions with the following exceptions. Tails were only homogenized with an 18.5-gauge needle 10 times before proceeding directly to the binding, washing and elution steps. Carrier RNA was not utilized.

RNA quality was assessed using the Agilent ScreenTape Assay (Agilent 5067-5579 and 5067-5580) and the Illumina TruSeq Stranded Total RNA kit with Ribo-Zero Gold (Illumina 20020598) was used for library preparation. Sequencing libraries were chemically denatured and applied to an Illumina NovaSeq flow cells using the NovaSeq XP chemistry workflow (Illumina 20021665). The flow cell was transferred to an Illumina NovaSeq instrument and a 2 x 150 cycle paired-end sequence run with 100 M reads was performed using a NovaSeq S2 reagent kit (Illumina 20012860). DESeq2 was used to perform differential gene expression analysis.[86] A heatmap of the top 40 differentially regulated genes was generated using RStudio. RNA sequences were visualized using integrated genomics viewer (IGV version 2.4.9).[87]

Whole-mount antibody staining

Immunofluorescence for activated Caspase-3 and phospho-histone H3 was performed as described.[88] Briefly, dechorionated, fixed and dehydrated 24-hpf embryos were washed at room temperature in 1X PDT (1X PBS, 0.1% Tween 20, 0.3% Triton X-, 1% DMSO) two times for 30 min and then transferred to blocking buffer (1X PBS, 0.1% Tween 20, 10% heat-inactivated fetal bovine serum, 2% BSA) for 1 h. Anti-activated Caspase 3 antibody (BD Biosciences 559,565) or anti-phospho-histone H3 antibody (Cell Signaling Technology 9701) was added at a 1:500 or 1:200 dilution for 2 h at room temperature, respectively. Embryos were washed in 1X PDT overnight at 4°C and transferred to blocking buffer the next day for 1 h at room temperature. Secondary anti-rabbit Alexa 568 antibody (Life Technologies A10042) was added at a 1:200 dilution for 2 h at room temperature; embryos were washed in 1X PDT overnight at 4°C and imaged the following day. Mutant *plrg1(hi3174aTg)* embryos display severe developmental cell death and were used as a positive control for the activated Caspase-3 assay.[89]

Protein lysates and western blotting

Wild-type embryos were microinjected with 3XFLAG-tagged mRNA constructs as described above. Ten embryos per condition were pooled at 24 hpf in 20 μL of RIPA buffer (150 mM NaCl, 50 mM Tris pH 8.0, 0.5% Deoxycholate, 1% NP-40, 0.1% SDS) supplemented with 0.7 mM PMSF and 1:100 of protease inhibitor cocktail (Sigma Aldrich P8340). Samples were homogenized and denatured at 95°C with 10 μL of 2X LSB/DTT (0.125 M Tris pH 6.8, 4% SDS, 20% glycerol, 0.005% bromophenol blue, 20 mM DTT). Samples were separated by SDS-PAGE, transferred to PVDF membranes (Millipore IPVH00010) using transfer buffer (1X Tris-Glycine buffer, 20% methanol, 0.1% SDS) for 1.5 h at 4°C. Membranes were blocked with 5% milk in PBST (1X PBS, 0.05% Tween 20) for 1 h at room temperature. Anti-Flag M2 (Sigma Aldrich F3165) primary antibody was added at 1:1000 and incubated overnight at 4°C. Membranes were washed 3X for 5 min each with PBST and incubated with anti-mouse-HRP (Jackson Immunoresearch 715-035-150) secondary antibody at 1:10,000 for 1 h at room temperature. Membranes were washed 3X for 5 min each with PBST and proteins were visualized by chemiluminescence detection (Thermo Fisher 34,095) using autoradiography film (Genesee Scientific 30-507).

CRISPR/Cas9

A sgRNA was designed against exon 2 of *gfi1b* (GRCz10 transcript 201) (agaatcacggaatcatgccacgg). sgRNA was made using the HiScribe T7 Quick High Yield RNA Synthesis RNA kit (NEB E2050S) and purified using the RNeasy Plus Mini kit (Qiagen 74,134) for small RNAs. sgRNA (400 ng/μL) and Cas9 (1000 ng/μL, IDT 1081058) were combined and injected into the single cell of zebrafish embryos. Injected embryos were grown to adults and genotyped to identify individuals with potential gfi1b exon 2 mutations. These adults were outcrossed to wild-type AB animals and progeny examined for transmission of *gfi1b* mutations. Adult F1 individuals were then outcrossed again to establish an F2 generation containing a deletion of 17 bp in exon 2 (Chr 21: 17295972-17295988) which was confirmed by DNA and RNA sequencing.

Image acquisition and processing

Both brightfield and fluorescent images were acquired on an Olympus SZX16 microscope with an aperture of 0.3 and configured with an Olympus DP74-CU camera. Embryos were imaged in 80% glycerol (WISH) or 4% methylcellulose (whole-mount antibody staining) on a 35-mm glass-bottom dish (Mattek Corporation P35G-1.0 20-C) at 4 to 5× magnification. Olympus cellSens Entry software was used for image acquisition. Adobe Illustrator CC 2017 and Adobe Photoshop CC 2017 were used to generate figures. The brightness/contrast of images was adjusted as indicated in the figure legends using Adobe Photoshop CC 2017.

Statistical analysis

The Wald test was used to determine statistical significance and the Benjamini-Hochberg test for false discovery rate in DESeq2.[86] An unpaired t-test with Welch's correction was performed using GraphPad Prism to determine if the number of phospho-histone H3 cells in the tail were significantly different between *lsd1* siblings.